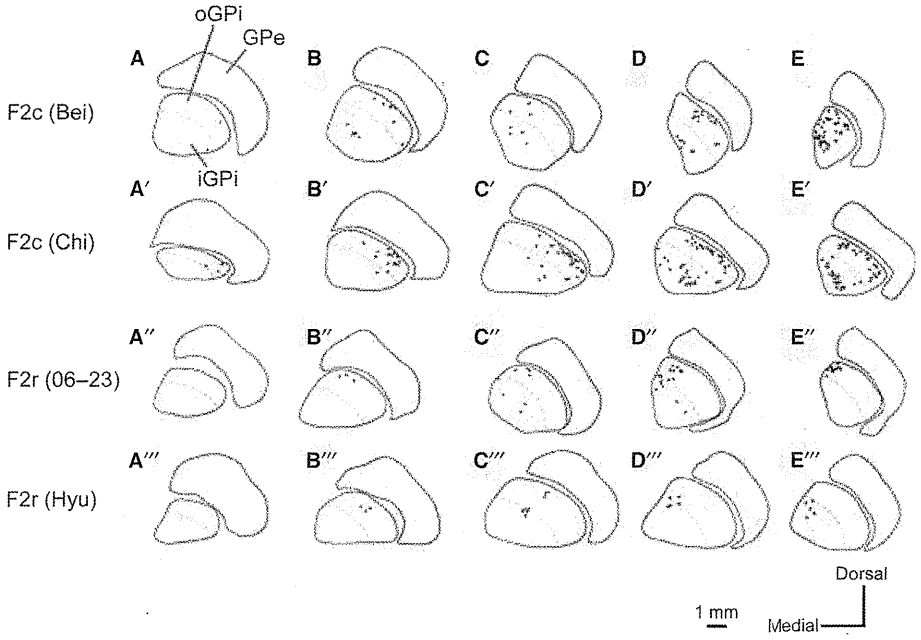

FIG. 3. Distribution of labeled neurons in the GPi. Five representative coronal sections are arranged rostrocaudally from left to right (A–E). Each row represents data from a single subject, as identified by the label on the left. The top two rows represent F2c injection, and the bottom two rows represent F2r injection. Each dot indicates the location of an infected neuron labeled by retrograde transneuronal transport (second-order neurons). Scale bar: 1 mm. oGPi, outer portion of GPi; iGPi, inner portion of GPi.

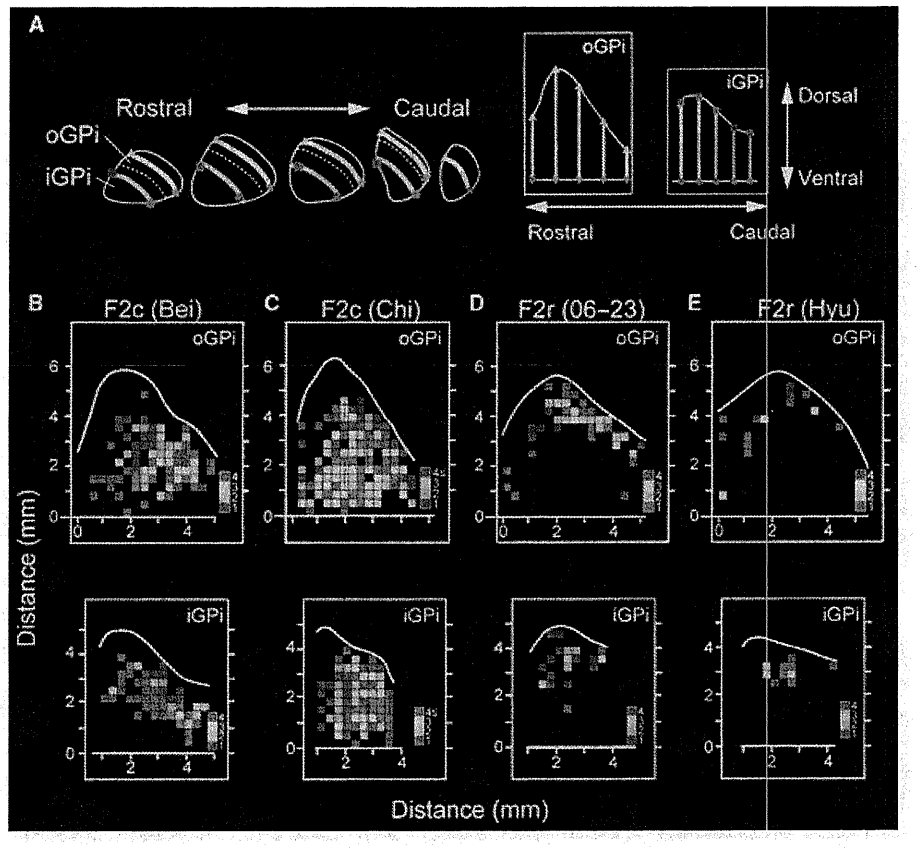

FIG. 4. Density maps of the GPi after F2 injection. (A) Procedures to construct two-dimensional density maps of the GPi. The unfolding process was begun by drawing a line through the center of the outer or inner portion of the GPi (top). The reference points were placed at the bottom (the pink star or the red circle) and the top (the cyan triangle or the blue square) of the GPi. The position of each labeled neuron was projected onto the central line. Then, each line through the nucleus was aligned on the ventral edge of the GPi (bottom). Neurons were divided into 300 × 300-μm bins. B and C show the conditions after F2c injection. D and E show the conditions after F2r injection. The top row presents maps of the outer portion. The bottom row presents maps of the inner portion. oGPi, outer portion of GPi; iGPi, inner portion of GPi.

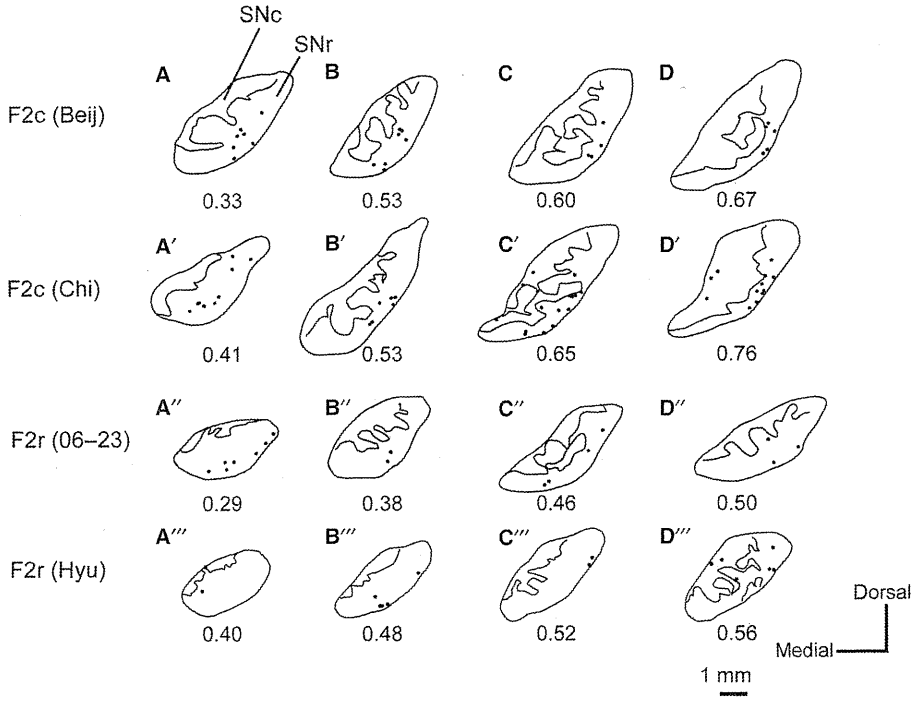

FIG. 5. Distribution of labeled neurons in the SNr. Four representative coronal sections are arranged rostrocaudally from left to right (A–D). Each dot indicates the location of a labeled neuron. Each row represents data from a single subject, as identified by the label on the left. The top two rows present the conditions after F2c injection, and the bottom two rows represent the conditions after F2r injection. The number attached to each section indicates its relative rostrocaudal position within the SNr (most rostral level = 0, most caudal level = 1). The lines in each section indicate the border between the SNr and the SNc, substantia nigra pars compacta. Scale bar: 1 mm.

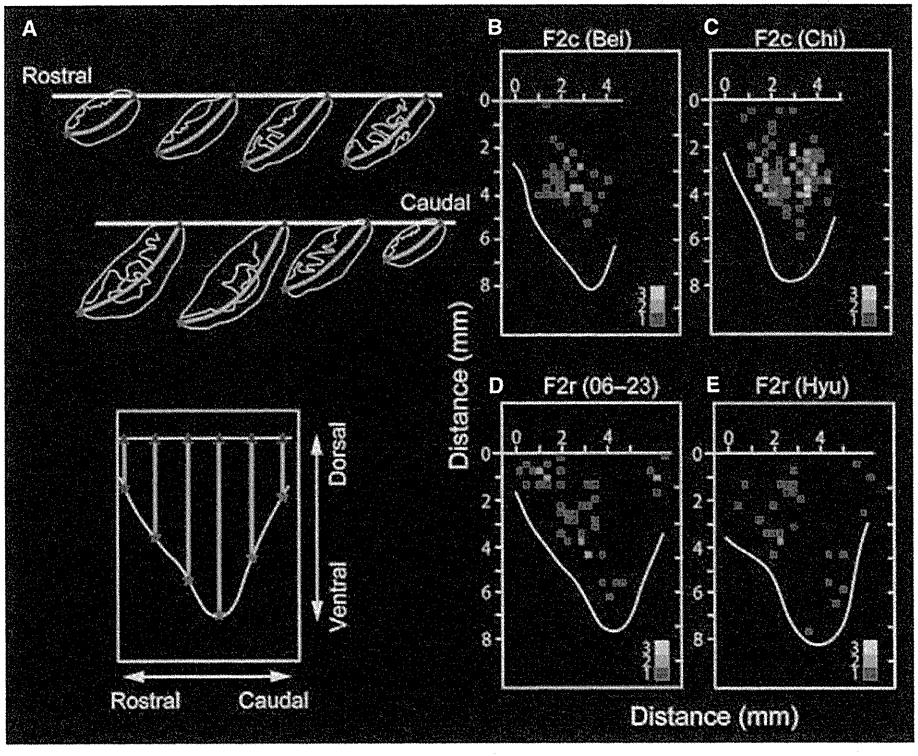

FIG. 6. Density maps of the SNr after F2 injection. (A) Procedures to construct two-dimensional density maps of the SNr. The unfolding process was begun by drawing a line through the center of the nucleus on each section. The reference points were placed at the medial edge (the red star) and the lateral edge (the blue triangle) of the SNr. The position of each labeled neuron was projected onto the central line. Then, each line through the nucleus was aligned on the lateral edge of the SNr (bottom). Neurons were divided into 300 × 300-μm bins. B and C show the neuronal density after F2c injection. D and E show the neuronal density after F2r injection.

GPe

Labeled neurons were widely distributed over the GPe following F2c injection, whereas labeled neurons occupied a more restricted area after the F2r injection (Figs 2C and 7). To compare the two distribution patterns in detail, we prepared two-dimensional density maps of the GPe to depict the results of F2c and F2r injections (Fig. 8A). After F2c injection, labeled neurons were found in the caudal and ventral portions as well as in the rostral and dorsal portions (Fig. 8B and C), whereas those after F2r injection were located in the rostral and dorsal portions of the GPe (Fig. 8D and E). These data indicated that the area in which GPe neurons projected multisynaptically to F2r was included within the area in which the GPe neurons projected to F2c.

The number of labeled neurons in the GPe after F2c injection was 623 on average (564 cells in Ams and 682 cells in Del), whereas this figure was 173 (202 cells in 06–22 and 144 cells in Itt) after F2r injection. The proportion of bins containing at least one labeled neuron was 60% on average (360 of 569 bins in Ams, and 329 of 567 bins in Del) after F2c injection (Fig. 8B and C), and the average proportion was 20% (145 of 677 bins in 06–22, and 109 of 550 bins in Itt) after F2r injection (Fig. 8D and E). These data indicated that F2c received input from the GPe that was three times as widely distributed as that received by F2r.

STN

Figure 9 shows the density map of the labeled neurons in the STN in each animal. After F2r injection, neuronal labeling was located primarily in the ventral aspect (Fig. 9, lower rows), whereas the zone of labeling following F2c injection involved that of labeling following F2r injection and expanded more dorsally (Fig. 9, upper rows). The number of labeled STN neurons after F2c injection was 276 on average (288 cells in Ams and 263 cells in Del), and the number after F2r injection was 75 on average (83 cells in 06–22 and 67 cells in Itt).

Striatum

Large numbers of labeled neurons were observed in the striatum. Labeled neurons were widely distributed in the striatal cell bridge region and in adjacent areas of the caudate nucleus and the putamen following each injection (Fig. 10). In addition, dense neuronal labeling was seen in the ventral striatum. The labeled striatal neurons following F2c injection greatly outnumbered those following F2r injection. The average numbers of labeled neurons were 13 679 (13 780 cells in Ams and 13 577 cells in Del) after F2c injection, and 3686 (3111 cells in 06–22 and 4260 cells in Itt) after F2r injection.

Discussion

We examined the organization of multisynaptic projections from the BG to F2 in macaques. After injections of rabies virus F2r and F2c, second-order neuron labeling occurred in the GPi and SNr. Subsequently, third-order neuron labeling was observed in the GPe, STN, and striatum. Analysis of the distribution of labeled neurons in each nucleus revealed several characteristics of the multisynaptic BG–F2 projections. We will discuss each of our findings individually below.

Segregation of GPi and SNr origins of multisynaptic F2c and F2r projections

Previous studies using retrograde trans-synaptic transport of neurotropic viruses have revealed that both the outer and the inner portions of the GPi consist of at least two distinct territories (i.e. motor and association territories) (Middleton and Strick, 2000a,b). The motor territory, occupying the caudoventral region of the GPi, projects multisynaptically to the primary motor cortex (M1), the supplementary motor area (SMA), and the ventral premotor area via the motor thalamus (Hoover & Strick, 1993, 1999; Akkal *et al.*, 2007). In contrast, the association territory, occupying the rostrodorsal region of

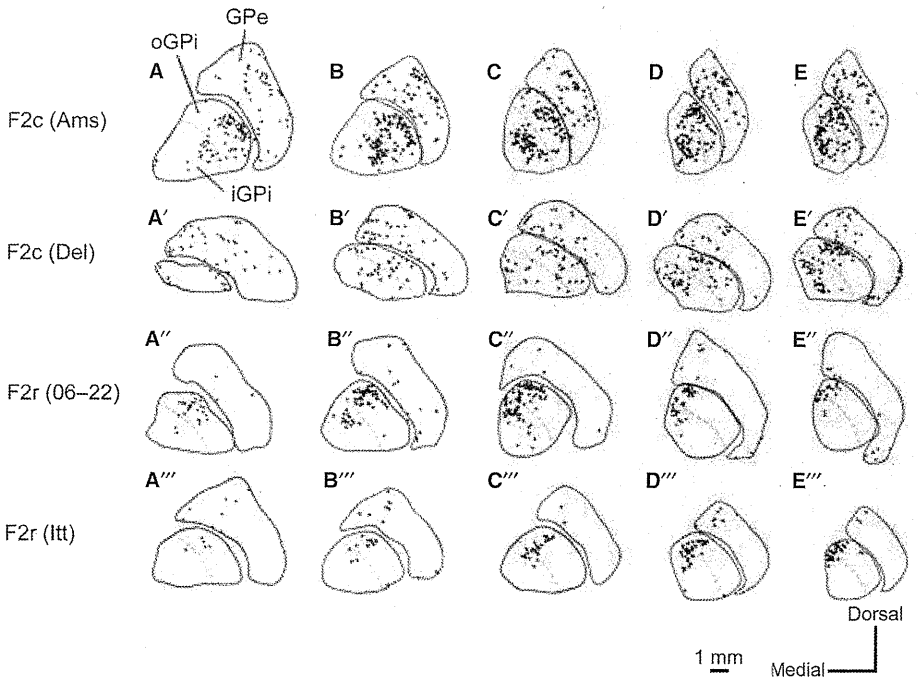

FIG. 7. Distribution of labeled neurons in the GPe (third-order neurons) and GPi (second-order or third-order neurons). Each row (A–E) represents data from a single subject, as identified by the label on the left. The top two rows represent the neuronal distribution following F2c injection, and the bottom two rows represent the neuronal distribution following F2r injections. Each dot indicates the location of an infected neuron. oGPi, outer portion of GPi; iGPi, inner portion of GPi.

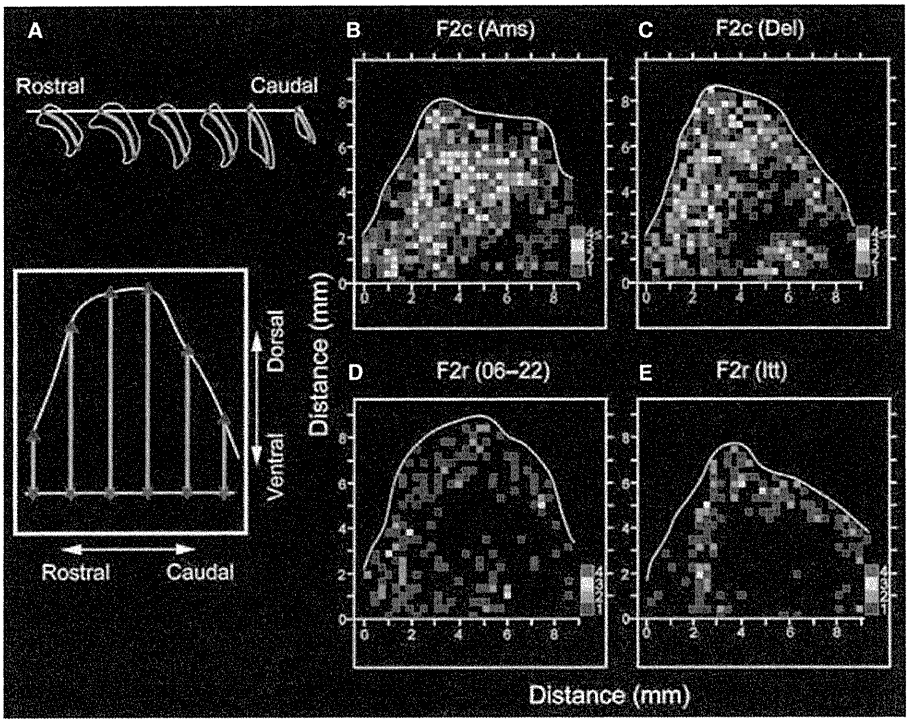

FIG. 8. Density maps of the GPe after F2 injection. (A) Procedures to construct two-dimensional density maps of the GPe. The unfolding process was begun by drawing a line through the center of the GPe (top). The reference points were placed at the bottom (the red star) and at the top (the blue triangle) of the GPe. The position of each labeled neuron was projected onto the central line. Then, each line through the nucleus was aligned on the ventral edge of the GPe (bottom). Neurons were divided into 300 × 300-μm bins. B and C show the neuronal density after F2c injection. D and E show the neuronal density after F2r injection.

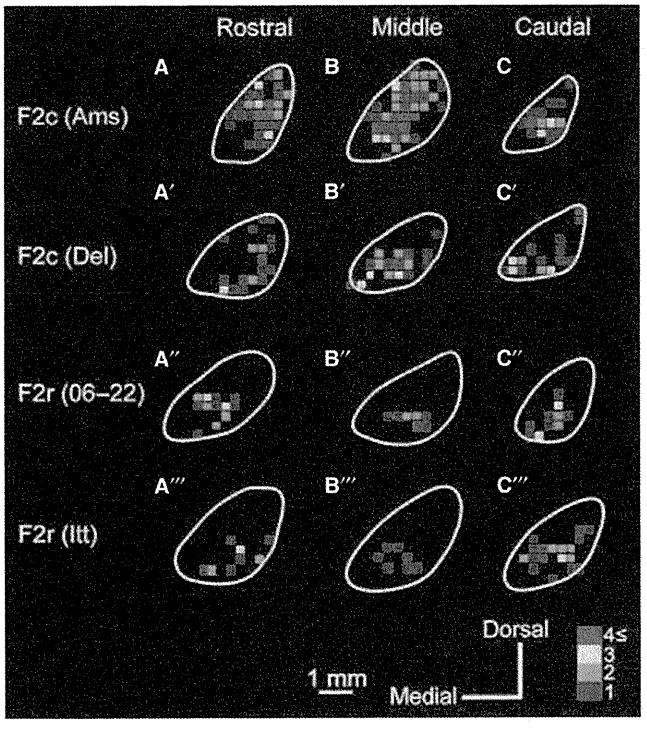

FIG. 9. Distribution of labeled neurons in the STN. Three coronal sections are arranged rostrocaudally from left to right (A–C). Each STN section was divided into 300 × 300-μm bins. The number of labeled neurons in each bin was counted and color-coded. Each row represents the data from a single subject, as identified by the label on the left. The top two rows show the neuronal distribution after F2c injection. The bottom two rows show the neuronal distribution after F2r injection. Scale bar: 1 mm.

the GPi, projects multisynaptically to the dorsal part of area 46 and the lateral part of area 9 in the prefrontal cortex and the pre-supplementary motor area (Middleton & Strick, 2002; Akkal *et al.*, 2007). This segregation between motor and association territories has also been revealed by electrical stimulation (Yoshida *et al.*, 1993).

In the present study, we found that neurons in the motor territory of the GPi constituted the major source of input to F2c. Comparison of the distribution of F2c-projecting neurons with that of SMA-projecting neurons (Akkal *et al.*, 2007) revealed that GPi neurons projecting multisynaptically to F2c tend to be located dorsal to those projecting to the SMA. Furthermore, we found that GPi neurons projecting multisynaptically to F2r were distributed in the dorsal part at the rostrocaudal middle level. According to the topographical map of the GPi, this region appears to be located just caudal to the association territory (Middleton & Strick, 2002; Akkal *et al.*, 2007), suggesting that it is situated in the transition zone between motor and association territories, which represent the calbindin-rich or calbindin-poor zone, respectively (Akkal *et al.*, 2007). Subsequently, by measuring the proportion of labeled bins, we confirmed that GPi neurons projecting multisynaptically to F2c were distributed more extensively than were those projecting to F2r. This indicates that the motor territory of the GPi is broader than its association territory.

It has been shown that the caudal and rostral parts of the dorsal premotor area in the cebus monkey (*Cebus apella*) receive input from the motor and nonmotor territories of the GPi, respectively (Dum *et al.*, 2004). Although this caudal part (caudal dorsal premotor area) corresponds to our F2c, the rostral dorsal premotor area used by Dum *et al.* (2004), which is located within area F7, is more rostral than our F2r. Following the injection of rabies into the caudal dorsal premotor area or F2c, retrograde neuron labeling was observed in the motor territory of the GPi, indicating that the basic architecture of the GPi–

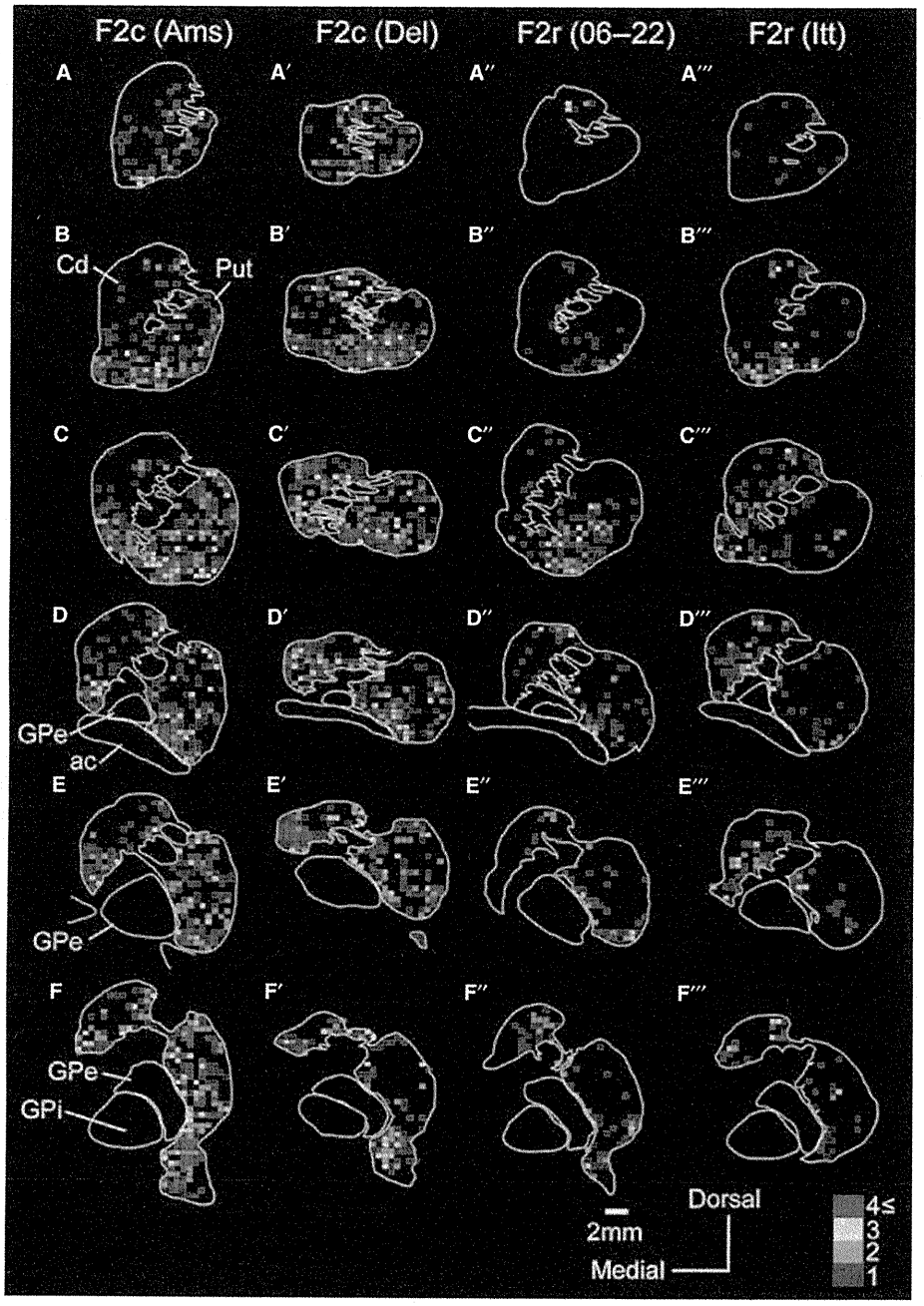

FIG. 10. Distribution patterns of neuronal labeling in the striatum 4 days after rabies injections into F2. Six equidistant coronal sections (3 mm apart) are arranged rostrocaudally from top to bottom (A–F). Each striatal section was divided into 500 × 500-μm bins. The number of labeled neurons in each bin was counted and color-coded. Each column represents the data from a single subject, as identified by the label on the top. The rostrocaudal level of the fourth row corresponds to that of the anterior commissure. The left two columns represent the neuronal distribution following F2c injection. The right two columns represent the neuronal distribution following F2r injection. Scale bar: 2 mm. ac, anterior commissure; Cd, caudate nucleus; Put, putamen.

F2c pathway in macaque monkeys is equivalent to that of the GPi–caudal dorsal premotor area pathway in cebus monkeys. Moreover, GPi neurons projecting multisynaptically to the rostral dorsal premotor area appeared to be located in a more rostral portion than those projecting to F2r (P. L. Strick, personal communication), suggesting that these two regions of the dorsal premotor area receive multisynaptic inputs from distinct portions of the GPi.

The topographical organization of another output nucleus, the SNr, was also revealed. The rostral and caudolateral portions of the SNr have been shown to project multisynaptically to prefrontal cortical areas, such as areas 46, 9, and 12 (Middleton & Strick, 2002). It has also been reported that the caudolateral portion of the SNr sends multisynaptic outputs to the frontal eye field and the superior colliculus (Beckstead *et al.*, 1981; Lynch *et al.*, 1994), suggesting that this portion is involved in oculomotor control (Hikosaka & Wurtz, 1983). Moreover, the caudolateral portion projects multisynaptically to the inferior temporal cortex, indicating that this portion plays an additional role in the processing of information about visual objects (Middleton & Strick, 1996b). In contrast, the most medial part of the SNr has been shown to receive inputs from the ventral striatum and the

ventral pallidum (Haber *et al.*, 1990, 1993). By injecting an anterograde tracer into the ventromedial portion of the GPe, where bicuculline microinjection caused stereotypy in monkeys, Francois *et al.* (2004) demonstrated that this region projected to the most medial part of the SNr at its rostral level. These findings suggest that the most medial part of the SNr belongs to a limbic circuit. Furthermore, it has been revealed that the sensorimotor territory of the striatum projects to the central part of the SNr (Francois *et al.*, 1994; Kaneda *et al.*, 2002). Taken together, these data elucidate the topographic organization of the SNr from a functional perspective.

In this study, we found that the caudocentral portion of the SNr projected multisynaptically to F2c. This SNr portion corresponds to the area that receives input from the SMA-recipient region of the striatum (Kaneda *et al.*, 2002). This suggests that another looping circuit may operate through the SNr in the service of motor control. By contrast, SNr neurons projecting multisynaptically to F2r were located in a more rostral portion, which has been shown to project to the prefrontal cortex (Middleton & Strick, 2002). However, the labeling in the caudolateral portion was meager, which is consistent with the observation that F2r is not involved in oculomotor control or in processing information about visual objects.

In summary, our results revealed that largely segregated parts of the GPi and SNr project multisynaptically to F2c and F2r. In general, F2c receives multisynaptic inputs from portions of the GPi and SNr that are interconnected with the cortical motor-related areas, whereas F2r receives multisynaptic inputs from the portions that are closely related to the prefrontal cortex.

Distribution of GPe and STN origins of multisynaptic F2c and F2r projections

Following a post-injection survival period of 4 days, the rabies virus injected into F2c or F2r was transported to the GPe, STN and striatum via the GPi and/or SNr. The existence of motor, association and limbic territories in the GPe has been suggested by a combination of anatomical and pathophysiological studies (Francois *et al.*, 2004; Grabli *et al.*, 2004). In the present study, GPe neurons labeled after F2c injection were widely distributed, with higher density in the rostral and dorsal portions, and those labeled after F2r injection were also located in the rostral and dorsal portions, albeit over a more restricted area. Furthermore, the F2r territory was observed to be included within the F2c territory. It has been reported that dual somatotopic maps exist in the medial and lateral parts of the STN. The medial part receives inputs from area 6 (i.e. the SMA and PMd), whereas the lateral portion receives input from area 4 (i.e. M1) (Nambu *et al.*, 1996, 1997; Kelly & Strick, 2004). It has also been shown that the ventral aspect of the STN is interconnected with the prefrontal cortex (Kelly & Strick, 2004). In our study, neurons projecting multisynaptically to F2c and F2r were intermingled, and we observed that the area containing F2r-projecting neurons tended to be included within the area containing F2c-projecting neurons. STN neurons labeled after F2c injection were distributed widely over both the medial and the lateral parts, indicating that F2c receives inputs from both of the dual somatotopic maps in the STN. In contrast, STN neurons projecting multisynaptically to F2r were found mainly in the ventral part, suggesting that F2r receives multisynaptic input from the association territory. Altogether, the basic network architecture of the GPi/SNr seems to differ from that of the GPe/STN. As the GPe and STN are the intermediate stations in the indirect pathways of the BG (Alexander & Crutcher, 1990), these findings suggest that the mode of information processing in the indirect pathway is essentially different from that in the direct pathway (i.e. the direct projections from the striatum to the GPi/SNr).

Intermingling of striatal origins of multisynaptic F2c and F2r projections

The striatum, the caudate nucleus and the putamen, receives input from various areas of the cerebral cortex. The caudate nucleus receives inputs primarily from the association areas in the frontal and parietal lobes (Yeterian & Van Hoesen, 1978; Selemon & Goldman-Rakic, 1985; Arikuni & Kubota, 1986; Saint-Cyr *et al.*, 1990; Yeterian & Pandya, 1991). By contrast, the putamen, especially its caudal aspect, receives inputs primarily from the sensorimotor areas, including various motor-related areas (Künzle, 1975, 1977; Flaherty & Graybiel, 1993b, 1994; Takada *et al.*, 1998a,b; Nambu *et al.*, 2002). Furthermore, the ventral striatum receives inputs from the medial and orbital prefrontal areas (Eblen & Graybiel, 1995; Haber *et al.*, 2006), the cingulate gyrus (Kunishio & Haber, 1994), the amygdala (Fudge *et al.*, 2002), and the hippocampal formation (Friedman *et al.*, 2002).

In the present study, both F2r and F2c injections led to neuronal labeling in the dorsal striatum, including the caudate nucleus and the putamen, as well as in the region of the striatal cell bridge. The region of the putamen that contained labeled neurons from F2c overlapped with the zone receiving direct input from F2c (Takada *et al.*, 1998a). This suggests the operation of an F2c–BG loop circuit. Although we have not identified a striatal region to which F2r sends projections, the rostral part of the dorsal premotor area has been shown to send projections to the dorsolateral region of the caudate nucleus and the dorsal, lateral and ventral regions of the putamen (Künzle, 1978). Our own study has also shown that area F7 projects to the region of the striatal cell bridge lying between the caudate nucleus and the putamen (Tachibana *et al.*, 2004). Thus, it is suggested that an F2r–BG loop circuit operates independently from the F2c–BG loop circuit. Additional labeled neurons were also found in widespread areas of the striatum after F2c and F2r injections. These labeled neurons were distributed in the dorsal and lateral aspects of the caudate nucleus, which receive extensive inputs from the prefrontal cortex (e.g. areas 46 and 9) (Kemp & Powell, 1970; Selemon & Goldman-Rakic, 1985; Calzavara *et al.*, 2007), and also in the medial and ventral aspects of the caudate nucleus and the ventromedial putamen, including the area caudal to the anterior commissure, which receives inputs from the limbic territories of the brain, such as the medial and orbital aspects of the prefrontal cortex, the amygdala, the hippocampal formation, and the agranular and dysgranular insular cortices (Selemon & Goldman-Rakic, 1985; Haber *et al.*, 1995, 2006; Fudge *et al.*, 2002, 2004, 2005; Friedman *et al.*, 2002; Kelly & Strick, 2004; Calzavara *et al.*, 2007). These results suggest that F2c and F2r both receive multisynaptic inputs from the association and limbic territories as well as from the striatal regions to which F2c and F2r, in turn, specifically project.

Yeterian & Van Hoesen (1978) originally proposed that two cortical regions linked via cortico-cortical connections send converging inputs to the striatum. Subsequently, Graybiel and colleagues demonstrated that M1 and the primary somatosensory cortex send converging inputs to the putamen, and that the frontal and supplementary eye fields send these to the caudate nucleus (Parthasarathy *et al.*, 1992; Flaherty & Graybiel, 1993b). Moreover, it has been shown that single striatal interneurons receive converging inputs from motor and sensory cortical areas (Bolam *et al.*, 2000; Ramanathan *et al.*, 2002), indicating the existence of a convergence of multiple interconnected cortical areas at the cellular level. Flaherty & Graybiel (1994) proposed that multiple patches within the striatal matrix receive diverging inputs

from a single cortical area and, in turn, send converging outputs to the GPi and GPe. Furthermore, it has been shown that projections from the anterior cingulate and obitofrontal cortices, carrying reward-related signals, spatially overlap with those from the dorsolateral prefrontal cortex, carrying cognitive signals, within the rostral striatum (Selemon & Goldman-Rakic, 1985; Haber *et al.*, 2006). Synthesis of these lines of evidence suggests that the striatum receives diverging inputs from a single cortical area and converging inputs from distinct, but anatomically related, cortical areas; it also suggests that outputs from spatially distributed striatal neurons reconverge at the level of the GPi. The present data are consistent with such a connectional framework, which displays the segregated distribution of GPi/SNr neurons projecting multisynaptically to F2c and F2r as well as the intermingled distribution of striatal neurons projecting multisynaptically to these areas. Given that F2 is characterized by widespread interconnections with cortical areas, including the motor territory (i.e. M1, the SMA, and the cingulate motor area), the association territory (i.e. the prefrontal cortex), and the limbic territory (i.e. the cingulate gyrus) (Barbas & Pandya, 1987; Luppino *et al.*, 2003), we suggest that F2 may receive multisynaptic inputs from the striatal regions that receive converging inputs from the cortical areas with which F2 is cortically interconnected.

In the current study, the number of rabies-labeled neurons was greater after F2c injection than after F2r injection, although the extent of the injection site was comparable between the two cases. This is probably ascribable to the fact that F2r is interconnected predominantly with areas in the frontal association cortex, whereas F2c is interconnected not only with these areas, but also with M1 (Barbas & Pandya, 1987; Luppino *et al.*, 2003). Therefore, it might be the case that F2c receives input not only from the association territory, but also from the motor territory of the BG, whereas F2r receives input mainly from the association territory. A greater number of neurons labeled after F2c injection was also seen for the ventral striatum. As previous studies have reported that M1 receives multisynaptic input from the ventral striatum, probably via the substantia innominata (Kelly & Strick, 2004; Miyachi *et al.*, 2006), it can be considered that the ventral striatum sends widespread projections indirectly to the frontal cortex, including M1 and F2. This implies that the ventral striatum may have broader impacts on the processing of not only cognitive, but also motor, information. Functionally, it has been shown that the effect of the expected reward amount is greater on neuronal activity in more caudal areas of the frontal association cortex (Roesch & Olson, 2003) that might receive ample multisynaptic inputs from the ventral striatum. It remains to be elucidated whether distinct portions, or distinct groups of neurons, in the ventral striatum project to the motor and association territories of the frontal cortex, and what kind of impact the ventral striatum has on neuronal activity therein.

Conclusions

As a result of our analysis of the distribution patterns of BG neurons projecting multisynaptically to F2c and F2r, we propose the operation of two separate channels, each of which projects multisynaptically to F2c and F2r at the output area of the BG (i.e. the GPi and SNr). We further propose that segregation may be obscured at the input area of the BG (i.e. the striatum), where neurons projecting multisynaptically to F2c and F2r intermingle (Fig. 11). These results indicate that each of the two parallel loops (i.e. the F2c–BG loop and the F2r–BG loop) collects diverse inputs from the motor and association territories with which F2c and F2r are cortically interconnected. Because pallidal and nigral neurons possess widespread dendritic trees (Yelnik *et al.*, 1984, 1987), the GPi and SNr may constitute the sites at which diverse inputs are sorted and integrated, enabling each of these to send outputs to F2c and F2r separately. On the other hand, the distribution pattern of neurons in the GPe and STN that project multisynaptically to F2c and F2r differs from that of neurons in the GPi and SNr; the F2r territory seems to be included within the F2c territory in the GPe and STN. This suggests that the mode of information processing in the GPe and STN differs from that in the GPi and SNr. Together with previous data showing the precise network architecture of each component of the BG (Hazrati & Parent, 1992; Bolam *et al.*, 2000; Parent *et al.*, 2000), the results obtained in the present study will provide a novel framework for understanding the mode of information processing in the cortico-BG loop circuits.

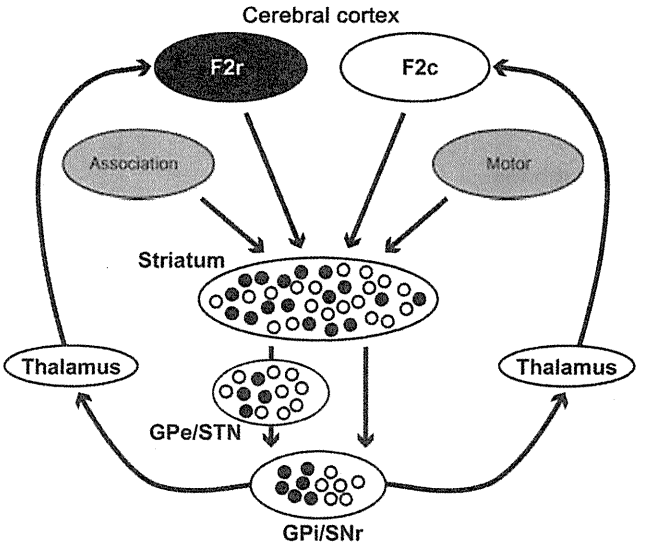

FIG. 11. A schematic diagram summarizing the results of the current study and presenting our hypothesis concerning the origins of multisynaptic projections to F2 from the BG. In the striatum, GPe/STN, and GPi/SNr, open and filled circles indicate neurons projecting multisynaptically to F2c and F2r, respectively. The arrow indicates the direction of the information flow through the cortico-BG loop circuits. Association, association areas in the cerebral cortex, such as the prefrontal cortex; Motor, motor-related areas in the cerebral cortex, such as M1 and the SMA. In the output stations of the BG (GPi/SNr), the cells of origin of multisynaptic projections to F2c and F2r are segregated. By contrast, intermingling rather than segregation is prominent with respect to the other BG components, including their input station (Striatum). Note that in GPe/STN, which connects the input and output stations, the F2r territory tends to be included within the F2c territory (see the text for details).

By analyzing the network linking F2 and the cerebellum, we revealed that the origins in the cerebellum of multisynaptic projections to F2c and F2r are segregated at the output station (i.e. the deep cerebellar nuclei), whereas both integration and segregation are evident in the cerebellar cortex (Hashimoto *et al.*, 2010). The networks connecting F2 and the BG/cerebellum may be governed by a common rule organizing the segregation at the output stage and the intermingling rather than the segregation at the input stage.

Acknowledgements

We wish to thank P. L. Strick for providing us with insightful comments on interpretation of the present data. We are grateful to M. Imanishi, Y. Ito, T. Kuroda, E. Mine, T. Ogata and K. Samejima for technical assistance. This work was supported by Grants-in-Aid for Scientific Research on Priority Areas (Integrative Brain Research) from the Ministry of Education, Culture, Sports,

Science and Technology of Japan (20019027 to E. Hoshi, 17021050 to M. Takada), a Grant-in-Aid for Young Scientists (S) from the Japan Society for the Promotion of Science (19670004), and a Career Development Award from the International Human Frontier Science Program Organization (E. Hoshi).

Abbreviations

BG, basal ganglia; F2, caudal aspect of the dorsal premotor area; F2c, caudal sector of the caudal aspect of the dorsal premotor area; F2r, rostral sector of the caudal aspect of the dorsal premotor area; GPe, external segment of the globus pallidus; GPi, internal segment of the globus pallidus; M1, primary motor cortex; SMA, supplementary motor area; SNr, substantia nigra pars reticulata; STN, subthalamic nucleus.

References

Akkal, D., Dum, R.P. & Strick, P.L. (2007) Supplementary motor area and presupplementary motor area: targets of basal ganglia and cerebellar output. *J. Neurosci.*, **27**, 10659–10673.

Alexander, G.E. & Crutcher, M.D. (1990) Functional architecture of basal ganglia circuits: neural substrates of parallel processing. *Trends Neurosci.*, **13**, 266–271.

Alexander, G.E., DeLong, M.R. & Strick, P.L. (1986) Parallel organization of functionally segregated circuits linking basal ganglia and cortex. *Annu. Rev. Neurosci.*, **9**, 357–381.

Arikuni, T. & Kubota, K. (1986) The organization of prefrontocaudate projections and their laminar origin in the macaque monkey: a retrograde study using HRP-gel. *J. Comp. Neurol.*, **244**, 492–510.

Barbas, H. & Pandya, D.N. (1987) Architecture and frontal cortical connections of the premotor cortex (area 6) in the rhesus monkey. *J. Comp. Neurol.*, **256**, 211–228.

Beckstead, R.M., Edwards, S.B. & Frankfurter, A. (1981) A comparison of the intranigral distribution of nigrotectal neurons labeled with horseradish peroxidase in the monkey, cat, and rat. *J. Neurosci.*, **1**, 121–125.

Bolam, J.P., Hanley, J.J., Booth, P.A. & Bevan, M.D. (2000) Synaptic organisation of the basal ganglia. *J. Anat.*, **196**(Pt 4), 527–542.

Brodmann, K. (1905) Beitrage zur histlogischen Lokalisation der Groshirnrinde. *J. Psychol. Neurol.*, **4**, 177–226.

Calzavara, R., Mailly, P. & Haber, S.N. (2007) Relationship between the corticostriatal terminals from areas 9 and 46, and those from area 8A, dorsal and rostral premotor cortex and area 24c: an anatomical substrate for cognition to action. *Eur. J. Neurosci.*, **26**, 2005–2024.

Caminiti, R., Ferraina, S. & Mayer, A.B. (1998) Visuomotor transformations: early cortical mechanisms of reaching. *Curr. Opin. Neurobiol.*, **8**, 753–761.

Cisek, P. & Kalaska, J.F. (2010) Neural mechanisms for interacting with a world full of action choices. *Annu. Rev. Neurosci.*, **33**, 269–298.

Cisek, P., Crammond, D.J. & Kalaska, J.F. (2003) Neural activity in primary motor and dorsal premotor cortex in reaching tasks with the contralateral versus ipsilateral arm. *J. Neurophysiol.*, **89**, 922–942.

Clower, D.M., Dum, R.P. & Strick, P.L. (2005) Basal ganglia and cerebellar inputs to 'AIP'. *Cereb. Cortex*, **15**, 913–920.

Draganski, B., Kherif, F., Kloppel, S., Cook, P.A., Alexander, D.C., Parker, G.J., Deichmann, R., Ashburner, J. & Frackowiak, R.S. (2008) Evidence for segregated and integrative connectivity patterns in the human basal ganglia. *J. Neurosci.*, **28**, 7143–7152.

Dum, R.P., Akkal, D. & Strick, P.L. (2004) The dorsal premotor area (PMd) and the pre-PMd area are the target of basal ganglia and cerebellar output in the cebus monkey. *Program No. 535.12. 2004 Neuroscience Meeting Planner*. San Diego, CA, Society for Neuroscience. http://www.sfn.org/absarchive/.

Eblen, F. & Graybiel, A.M. (1995) Highly restricted origin of prefrontal cortical inputs to striosomes in the macaque monkey. *J. Neurosci.*, **15**, 5999–6013.

Flaherty, A.W. & Graybiel, A.M. (1993a) Output architecture of the primate putamen. *J. Neurosci.*, **13**, 3222–3237.

Flaherty, A.W. & Graybiel, A.M. (1993b) Two input systems for body representations in the primate striatal matrix: experimental evidence in the squirrel monkey. *J. Neurosci.*, **13**, 1120–1137.

Flaherty, A.W. & Graybiel, A.M. (1994) Input–output organization of the sensorimotor striatum in the squirrel monkey. *J. Neurosci.*, **14**, 599–610.

Francois, C., Yelnik, J., Percheron, G. & Fenelon, G. (1994) Topographic distribution of the axonal endings from the sensorimotor and associative striatum in the macaque pallidum and substantia nigra. *Exp. Brain Res.*, **102**, 305–318.

Francois, C., Grabli, D., McCairn, K., Jan, C., Karachi, C., Hirsch, E.C., Feger, J. & Tremblay, L. (2004) Behavioural disorders induced by external globus pallidus dysfunction in primates II. Anatomical study. *Brain*, **127**, 2055–2070.

Friedman, D.P., Aggleton, J.P. & Saunders, R.C. (2002) Comparison of hippocampal, amygdala, and perirhinal projections to the nucleus accumbens: combined anterograde and retrograde tracing study in the macaque brain. *J. Comp. Neurol.*, **450**, 345–365.

Fudge, J.L., Kunishio, K., Walsh, P., Richard, C. & Haber, S.N. (2002) Amygdaloid projections to ventromedial striatal subterritories in the primate. *Neuroscience*, **110**, 257–275.

Fudge, J.L., Breitbart, M.A. & McClain, C. (2004) Amygdaloid inputs define a caudal component of the ventral striatum in primates. *J. Comp. Neurol.*, **476**, 330–347.

Fudge, J.L., Breitbart, M.A., Danish, M. & Pannoni, V. (2005) Insular and gustatory inputs to the caudal ventral striatum in primates. *J. Comp. Neurol.*, **490**, 101–118.

Grabli, D., McCairn, K., Hirsch, E.C., Agid, Y., Feger, J., Francois, C. & Tremblay, L. (2004) Behavioural disorders induced by external globus pallidus dysfunction in primates: I. Behavioural study. *Brain*, **127**, 2039–2054.

Graybiel, A.M. (2008) Habits, rituals, and the evaluative brain. *Annu. Rev. Neurosci.*, **31**, 359–387.

Haber, S.N., Lynd, E., Klein, C. & Groenewegen, H.J. (1990) Topographic organization of the ventral striatal efferent projections in the rhesus monkey: an anterograde tracing study. *J. Comp. Neurol.*, **293**, 282–298.

Haber, S.N., Lynd-Balta, E. & Mitchell, S.J. (1993) The organization of the descending ventral pallidal projections in the monkey. *J. Comp. Neurol.*, **329**, 111–128.

Haber, S.N., Kunishio, K., Mizobuchi, M. & Lynd-Balta, E. (1995) The orbital and medial prefrontal circuit through the primate basal ganglia. *J. Neurosci.*, **15**, 4851–4867.

Haber, S.N., Kim, K.S., Mailly, P. & Calzavara, R. (2006) Reward-related cortical inputs define a large striatal region in primates that interface with associative cortical connections, providing a substrate for incentive-based learning. *J. Neurosci.*, **26**, 8368–8376.

Hashimoto, M., Takahara, D., Hirata, Y., Inoue, K.I., Miyachi, S., Nambu, A., Tanji, J., Takada, M. & Hoshi, E. (2010) Motor and non-motor projections from the cerebellum to rostrocaudally distinct sectors of the dorsal premotor cortex in macaques. *Eur. J. Neurosci.*, **31**, 1402–1413.

Hazrati, L.N. & Parent, A. (1992) Convergence of subthalamic and striatal efferents at pallidal level in primates: an anterograde double-labeling study with biocytin and PHA-L. *Brain Res.*, **569**, 336–340.

Hikosaka, O. & Wurtz, R.H. (1983) Visual and oculomotor functions of monkey substantia nigra pars reticulata. I. Relation of visual and auditory responses to saccades. *J. Neurophysiol.*, **49**, 1230–1253.

Hoover, J.E. & Strick, P.L. (1993) Multiple output channels in the basal ganglia. *Science*, **259**, 819–821.

Hoover, J.E. & Strick, P.L. (1999) The organization of cerebellar and basal ganglia outputs to primary motor cortex as revealed by retrograde transneuronal transport of herpes simplex virus type 1. *J. Neurosci.*, **19**, 1446–1463.

Hoshi, E. & Tanji, J. (2006) Differential involvement of neurons in the dorsal and ventral premotor cortex during processing of visual signals for action planning. *J. Neurophysiol.*, **95**, 3596–3616.

Hoshi, E. & Tanji, J. (2007) Distinctions between dorsal and ventral premotor areas: anatomical connectivity and functional properties. *Curr. Opin. Neurobiol.*, **17**, 234–242.

Inase, M., Sakai, S.T. & Tanji, J. (1996) Overlapping corticostriatal projections from the supplementary motor area and the primary motor cortex in the macaque monkey: an anterograde double-labeling study. *J. Comp. Neurol.*, **373**, 283–296.

Inase, M., Tokuno, H., Nambu, A., Akazawa, T. & Takada, M. (1999) Corticostriatal and corticosubthalamic input zones from the presupplementary motor area in the macaque monkey: comparison with the input zones from the supplementary motor area. *Brain Res.*, **833**, 191–201.

Kaneda, K., Nambu, A., Tokuno, H. & Takada, M. (2002) Differential processing patterns of motor information via striatopallidal and striatonigral projections. *J. Neurophysiol.*, **88**, 1420–1432.

Kelly, R.M. & Strick, P.L. (2003) Cerebellar loops with motor cortex and prefrontal cortex of a nonhuman primate. *J. Neurosci.*, **23**, 8432–8444.

Kelly, R.M. & Strick, P.L. (2004) Macro-architecture of basal ganglia loops with the cerebral cortex: use of rabies virus to reveal multisynaptic circuits. *Prog. Brain Res.*, **143**, 449–459.

Kemp, J.M. & Powell, T.P. (1970) The cortico–striate projection in the monkey. *Brain*, **93**, 525–546.

Kunishio, K. & Haber, S.N. (1994) Primate cingulostriatal projection: limbic striatal versus sensorimotor striatal input. *J. Comp. Neurol.*, **350**, 337–356.

Künzle, H. (1975) Bilateral projections from precentral motor cortex to the putamen and other parts of the basal ganglia. An autoradiographic study in Macaca fascicularis. *Brain Res.*, **88**, 195–209.

Künzle, H. (1977) Projections from the primary somatosensory cortex to basal ganglia and thalamus in the monkey. *Exp. Brain Res.*, **30**, 481–492.

Künzle, H. (1978) An autoradiographic analysis of the efferent connections from premotor and adjacent prefrontal regions (areas 6 and 9) in macaca fascicularis. *Brain Behav. Evol.*, **15**, 185–234.

Lichter, D.G. & Cummings, J.L. (2001) *Frontal–Subcortical Circuits in Psychiatric and Neurological Disorders*. The Guilford Press, New York.

Luppino, G., Rozzi, S., Calzavara, R. & Matelli, M. (2003) Prefrontal and agranular cingulate projections to the dorsal premotor areas F2 and F7 in the macaque monkey. *Eur. J. Neurosci.*, **17**, 559–578.

Lynch, J.C., Hoover, J.E. & Strick, P.L. (1994) Input to the primate frontal eye field from the substantia nigra, superior colliculus, and dentate nucleus demonstrated by transneuronal transport. *Exp. Brain Res.*, **100**, 181–186.

Matelli, M., Luppino, G. & Rizzolatti, G. (1985) Patterns of cytochrome oxidase activity in the frontal agranular cortex of the macaque monkey. *Behav. Brain Res.*, **18**, 125–136.

Matelli, M., Govoni, P., Galletti, C., Kutz, D.F. & Luppino, G. (1998) Superior area 6 afferents from the superior parietal lobule in the macaque monkey. *J. Comp. Neurol.*, **402**, 327–352.

Middleton, F.A. & Strick, P.L. (1996a) Basal ganglia and cerebellar output influences non-motor function. *Mol. Psychiatry*, **1**, 429–433.

Middleton, F.A. & Strick, P.L. (1996b) The temporal lobe is a target of output from the basal ganglia. *Proc. Natl. Acad. Sci. USA*, **93**, 8683–8687.

Middleton, F.A. & Strick, P.L. (2000a) Basal ganglia and cerebellar loops: motor and cognitive circuits. *Brain Res. Brain Res. Rev.*, **31**, 236–250.

Middleton, F.A. & Strick, P.L. (2000b) Basal ganglia output and cognition: evidence from anatomical, behavioral, and clinical studies. *Brain Cogn.*, **42**, 183–200.

Middleton, F.A. & Strick, P.L. (2002) Basal-ganglia 'projections' to the prefrontal cortex of the primate. *Cereb. Cortex*, **12**, 926–935.

Miyachi, S., Lu, X., Inoue, S., Iwasaki, T., Koike, S., Nambu, A. & Takada, M. (2005) Organization of multisynaptic inputs from prefrontal cortex to primary motor cortex as revealed by retrograde transneuronal transport of rabies virus. *J. Neurosci.*, **25**, 2547–2556.

Miyachi, S., Lu, X., Imanishi, M., Sawada, K., Nambu, A. & Takada, M. (2006) Somatotopically arranged inputs from putamen and subthalamic nucleus to primary motor cortex. *Neurosci. Res.*, **56**, 300–308.

Nambu, A., Takada, M., Inase, M. & Tokuno, H. (1996) Dual somatotopical representations in the primate subthalamic nucleus: evidence for ordered but reversed body–map transformations from the primary motor cortex and the supplementary motor area. *J. Neurosci.*, **16**, 2671–2683.

Nambu, A., Tokuno, H., Inase, M. & Takada, M. (1997) Corticosubthalamic input zones from forelimb representations of the dorsal and ventral divisions of the premotor cortex in the macaque monkey: comparison with the input zones from the primary motor cortex and the supplementary motor area. *Neurosci. Lett.*, **239**, 13–16.

Nambu, A., Kaneda, K., Tokuno, H. & Takada, M. (2002) Organization of corticostriatal motor inputs in monkey putamen. *J. Neurophysiol.*, **88**, 1830–1842.

Parent, A., Sato, F., Wu, Y., Gauthier, J., Levesque, M. & Parent, M. (2000) Organization of the basal ganglia: the importance of axonal collateralization. *Trends Neurosci.*, **23**, S20–S27.

Parthasarathy, H.B., Schall, J.D. & Graybiel, A.M. (1992) Distributed but convergent ordering of corticostriatal projections: analysis of the frontal eye field and the supplementary eye field in the macaque monkey. *J. Neurosci.*, **12**, 4468–4488.

Ramanathan, S., Hanley, J.J., Deniau, J.M. & Bolam, J.P. (2002) Synaptic convergence of motor and somatosensory cortical afferents onto GABAergic interneurons in the rat striatum. *J. Neurosci.*, **22**, 8158–8169.

Roesch, M.R. & Olson, C.R. (2003) Impact of expected reward on neuronal activity in prefrontal cortex, frontal and supplementary eye fields and premotor cortex. *J. Neurophysiol.*, **90**, 766–789.

Saint-Cyr, J.A., Ungerleider, L.G. & Desimone, R. (1990) Organization of visual cortical inputs to the striatum and subsequent outputs to the pallido–nigral complex in the monkey. *J. Comp. Neurol.*, **298**, 129–156.

Selemon, L.D. & Goldman-Rakic, P.S. (1985) Longitudinal topography and interdigitation of corticostriatal projections in the rhesus monkey. *J. Neurosci.*, **5**, 776–794.

Tachibana, Y., Nambu, A., Hatanaka, N., Miyachi, S. & Takada, M. (2004) Input–output organization of the rostral part of the dorsal premotor cortex, with special reference to its corticostriatal projection. *Neurosci. Res.*, **48**, 45–57.

Takada, M., Tokuno, H., Nambu, A. & Inase, M. (1998a) Corticostriatal input zones from the supplementary motor area overlap those from the contra- rather than ipsilateral primary motor cortex. *Brain Res.*, **791**, 335–340.

Takada, M., Tokuno, H., Nambu, A. & Inase, M. (1998b) Corticostriatal projections from the somatic motor areas of the frontal cortex in the macaque monkey: segregation versus overlap of input zones from the primary motor cortex, the supplementary motor area, and the premotor cortex. *Exp. Brain Res.*, **120**, 114–128.

Takada, M., Tokuno, H., Hamada, I., Inase, M., Ito, Y., Imanishi, M., Hasegawa, N., Akazawa, T., Hatanaka, N. & Nambu, A. (2001) Organization of inputs from cingulate motor areas to basal ganglia in macaque monkey. *Eur. J. Neurosci.*, **14**, 1633–1650.

Wise, S.P. (1985) The primate premotor cortex: past, present, and preparatory. *Annu. Rev. Neurosci.*, **8**, 1–19.

Yelnik, J., Percheron, G. & Francois, C. (1984) A Golgi analysis of the primate globus pallidus. II. Quantitative morphology and spatial orientation of dendritic arborizations. *J. Comp. Neurol.*, **227**, 200–213.

Yelnik, J., Francois, C., Percheron, G. & Heyner, S. (1987) Golgi study of the primate substantia nigra. I. Quantitative morphology and typology of nigral neurons. *J. Comp. Neurol.*, **265**, 455–472.

Yeterian, E.H. & Pandya, D.N. (1991) Prefrontostriatal connections in relation to cortical architectonic organization in rhesus monkeys. *J. Comp. Neurol.*, **312**, 43–67.

Yeterian, E.H. & Van Hoesen, G.W. (1978) Cortico–striate projections in the rhesus monkey: the organization of certain cortico–caudate connections. *Brain Res.*, **139**, 43–63.

Yoshida, S., Nambu, A. & Jinnai, K. (1993) The distribution of the globus pallidus neurons with input from various cortical areas in the monkeys. *Brain Res.*, **611**, 170–174.

EJN fens EUROPEAN JOURNAL OF NEUROSCIENCE

European Journal of Neuroscience, Vol. 31, pp. 1402–1413, 2010 doi:10.1111/j.1460-9568.2010.07151.x

NEUROSYSTEMS

Motor and non-motor projections from the cerebellum to rostrocaudally distinct sectors of the dorsal premotor cortex in macaques

Masashi Hashimoto,[1,*] Daisuke Takahara,[2,3,4,*] Yoshihiro Hirata,[2,3,*] Ken-ichi Inoue,[2,3,*] Shigehiro Miyachi,[5] Atsushi Nambu,[4] Jun Tanji,[1] Masahiko Takada[2,3] and Eiji Hoshi[1]

[1]Tamagawa University Brain Science Institute, Machida, Tokyo 194-8610, Japan

[2]Department of System Neuroscience, Tokyo Metropolitan Institute for Neuroscience, Tokyo Metropolitan Organization for Medical Research, Fuchu, Tokyo, Japan

[3]Systems Neuroscience Section, Primate Research Institute, Kyoto University, Inuyama, Japan

[4]Division of System Neurophysiology, National Institute for Physiological Sciences and Department of Physiological Sciences, Graduate University for Advanced Studies (SOKENDAI), Myodaiji, Okazaki, Japan

[5]Cognitive Neuroscience Section, Primate Research Institute, Kyoto University, Inuyama, Japan

Keywords: CVS-11, motor cortex, rabies virus, transneuronal transport

Abstract

In the caudal part of the dorsal premotor cortex of macaques (area F2), both anatomical and physiological studies have identified two rostrocaudally separate sectors. The rostral sector (F2r) is located medial to the genu of the arcuate sulcus, and the caudal sector (F2c) is located lateral to the superior precentral dimple. Here we examined the sites of origin of projections from the cerebellum to F2r and F2c. We applied retrograde transsynaptic transport of a neurotropic virus, CVS-11 of rabies virus, in macaque monkeys. Three days after rabies injections into F2r or F2c, neuronal labeling was found in the deep cerebellar nuclei mainly of the contralateral hemisphere. After the F2r injection, labeled cells were distributed primarily in the caudoventral portion of the dentate nucleus, whereas cells labeled after the F2c injection were distributed in the rostrodorsal portion of the dentate nucleus, and in the interpositus and fastigial nuclei. Four days after rabies injections, Purkinje cells were densely labeled in the lateral part of the cerebellar cortex. After the F2r injection, Purkinje cell labeling was confined to Crus I and II, whereas the labeling seen after the F2c injection was located broadly from lobules III to VIII, including Crus I and II. These results have revealed that F2c receives inputs from broader areas of the cerebellum than F2r, and that distinct portions of the deep cerebellar nuclei and the cerebellar cortex send major projections to F2r and F2c, suggesting that F2c and F2r may be under specific influences of the cerebellum.

Introduction

The cerebellum plays a central role in executing a motor act in a smooth and coordinated manner through its major connections with the cerebral cortex and the spinal cord (Ito, 1984; Thach *et al.*, 1992; Kawato, 1999). With regard to the network that links the cerebellum and the cerebral cortex, a novel tract-tracing method by means of transsynaptic transport of neurotropic viruses (Ugolini *et al.*, 1987, 1989; Kuypers & Ugolini, 1990; Kelly & Strick, 2003; Miyachi *et al.*, 2005; Callaway, 2008) has revealed that the output from the cerebellum reaches the frontal lobe, including the primary motor cortex and the prefrontal cortex (Middleton & Strick, 1994, 2001; Kelly & Strick, 2003). A series of studies further suggest that each cortical area forms a separate closed loop circuit with the cerebellum (Hoover & Strick, 1999; Kelly & Strick, 2003; Clower *et al.*, 2005; Akkal *et al.*, 2007). By synthesizing a large set of data, Strick *et al.* have identified the motor and non-motor domains in the cerebellum; the motor domain is linked predominantly with the primary motor cortex, whereas the non-motor domain is not linked with the primary motor cortex, but with association cortical areas, such as the prefrontal cortex (for review, see Strick *et al.*, 2009).

The present study focuses on the origin of cerebellar projections to the dorsal premotor cortex (PMd) in Brodmann's area 6 of macaques (Brodmann, 1909; Wise, 1985; Barbas & Pandya, 1987). We previously recorded neuronal activity from PMd while monkeys were performing an arm-reaching task, and found that neurons displaying activity in relation to the process of motor planning and preparation were located mainly in the caudal part of PMd (Hoshi & Tanji, 2006) that coincides well with area F2 defined by cytochrome oxidase staining (Matelli *et al.*, 1985, 1991). Further, our results demonstrated that the properties of neuronal responses were different in the rostral and caudal sectors of area F2 (F2r and F2c) that lie medial to the genu of the arcuate sulcus and lateral to the superior precentral dimple, respectively.

Correspondence: Dr E. Hoshi, as above.
E-mail: hoshie@lab.tamagawa.ac.jp

*M.H., D.T., Y.H. and K-i. I. authors contributed equally to this work.

Received 29 September 2009, revised 25 January 2010, accepted 26 January 2010

TABLE 1. Summary of experiments

Monkey	Species	Injection site	Survival (days)	Injection tracks (n)	Injection volume (μL)
Hyu	*Macaca mulatta*	F2r	3	3	3.0
06–23	*Macaca fuscata*	F2r	3	3	3.0
06–22	*M. fuscata*	F2r	4	3	3.0
Itt	*M. fuscata*	F2r	4	3	3.0
Bei	*M. fuscata*	F2c	3	4	4.0
Chi	*M. fuscata*	F2c	3	4	4.0
Ams	*M. fuscata*	F2c	4	4	4.0
Del	*M. fuscata*	F2c	4	4	4.0

It has been shown that the caudal (area F2) and rostral (area F7) parts of PMd in the cebus monkey (*Cebus apella*) receive input from the motor or non-motor domain of the deep cerebellar nuclei, respectively (Dum *et al.*, 2002, 2004). However, given the differential functional specificities in areas F2r and F2c, it is of importance to investigate the origins of projections from the cerebellum to F2r vs. F2c in macaque monkeys that have been widely used for exploration of neural mechanisms underlying motor control. Here we show that distinct portions of the deep cerebellar nuclei and the cerebellar cortex send major projections to F2r and F2c. These results suggest that F2r and F2c in the caudal PMd may be involved in planning and executing voluntary movements under specific influences of the cerebellum.

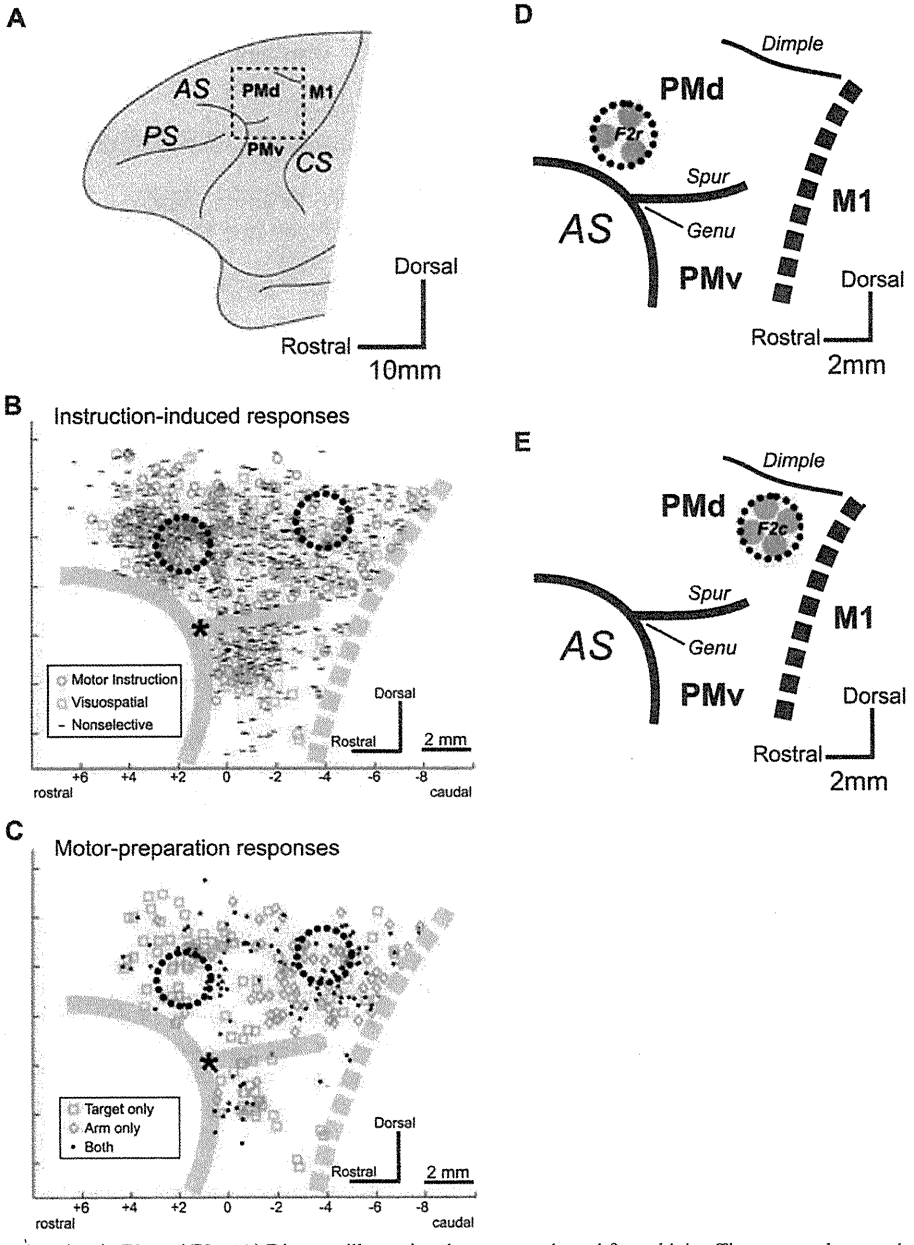

FIG. 1. Locations of the injection sites in F2r and F2c. (A) Diagram illustrating the macaque lateral frontal lobe. The rectangular area drawn with broken lines in (A) is enlarged in (B–E). (B) and (C) Distributions of neuronal activity found in prior single-neuron recordings. Two panels were adopted from Hoshi & Tanji (2006). (B) The location of cells whose activity reflected the motor instruction (circle) or visuospatial feature of visual signals (square) after an instruction cue was presented. (C) The location of cells whose activity reflected only target location (square), only left- or right-arm use (diamond), or both target location and arm use (dot). In each panel, the distributions of neuronal response properties were different in the rostral and caudal parts. Two circles drawn with broken lines indicate the intended injection sites in F2r and F2c, respectively. (D) and (E) Injection sites of rabies virus in F2r (D) and F2c (E). Within each site, small circles in gray (0.5 mm in radius) indicate the estimated viral spread around the injection tracks. (B–E) The border between the premotor cortex (PMd, dorsal premotor cortex; PMv, ventral premotor cortex) and the primary motor cortex (M1) is represented with the broken line. The genu of the arcuate sulcus (AS) is denoted with asterisks in (B) and (C). CS, central sulcus; Dimple, superior precentral dimple; PS, principal sulcus; Spur, spur of AS.

Materials and methods

Animals

We used seven Japanese (*Macaca fuscata*) monkeys and one rhesus (*Macaca mulatta*) monkey of either sex weighing 4.0–7.6 kg (Table 1). The experimental protocol was approved by the Animal Care and Use Committee of the Tokyo Metropolitan Institute for Neuroscience, and all experiments were conducted in accordance with the Tokyo Metropolitan Institute for Neuroscience Guidelines for the Care and Use of Animals (2000).

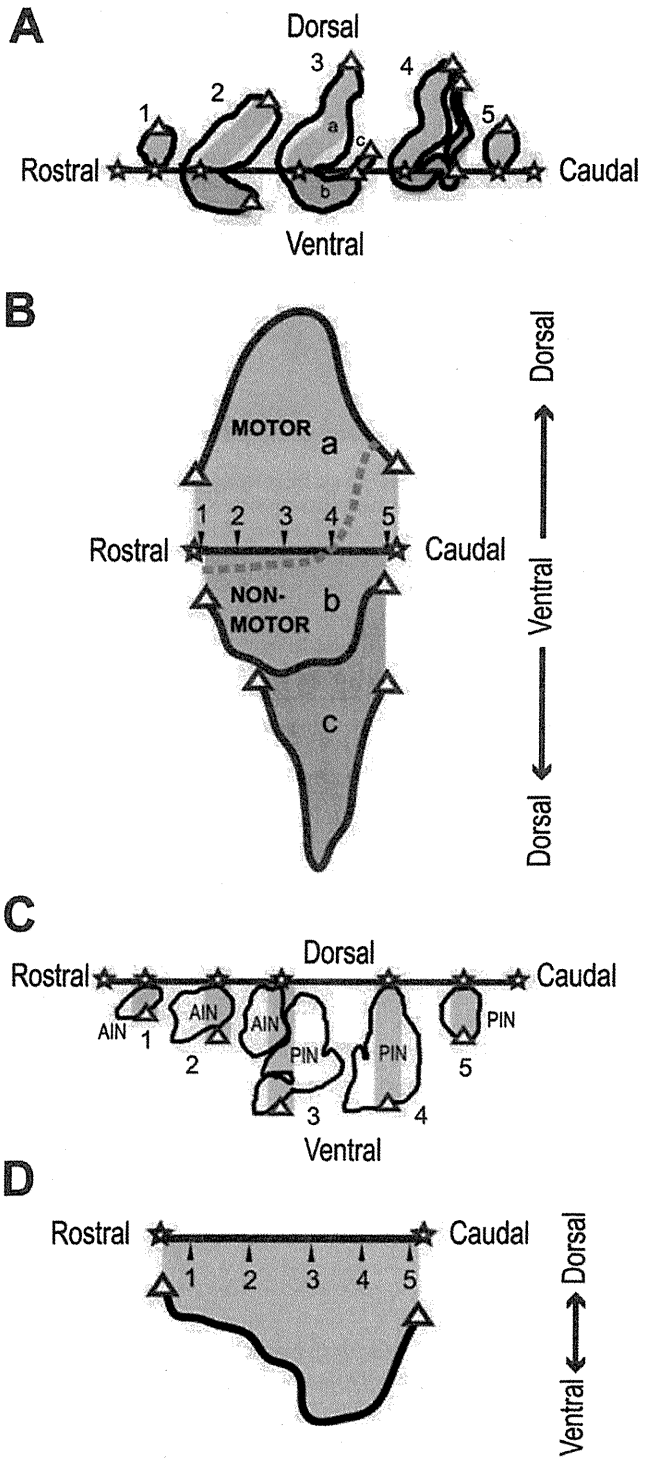

Surgical procedures

A general anesthesia of the monkeys was induced with ketamine hydrochloride (10 mg/kg, i.m.) and maintained with sodium pentobarbital (20 mg/kg, i.v.). During the surgical operation, hydration was maintained with lactated Ringer's solution (i.v.). An antibiotic (Rocephin; 75 mg/kg, i.m.) was administered at the time of initial anesthesia. The monkey's head was secured in a stereotaxic frame, and the skin and muscle were retracted to expose the skull over the left hemisphere. A large craniotomy was made over the left frontal lobe, and the dura mater was cut to expose the superior limb of the arcuate sulcus, the genu of the arcuate sulcus, the superior precentral dimple and the central sulcus, which allowed us to visually inspect the injection sites on the cortical surface. In three of the eight monkeys, we administered dexamethasone (Decadron; 0.5 mg/kg, i.m.) because they showed a sign of slight swelling of the exposed area. Soon after the administration, the cortex returned to normal conditions. After confirming this, we started viral injections.

Viral injections

The virus was derived from the Center for Disease Control and Prevention (Atlanta, GA, USA) and donated by Dr Satoshi Inoue (The National Institute of Infectious Disease, Tokyo, Japan). The titer of a stock viral suspension was 1.4×10^8 focus-forming units/mL. The location of each injection site was based on surface landmarks and their known relationship to the caudal sector of the dorsal premotor area (area F2; Matelli *et al.*, 1985). Injection sites of the rostral sector of area F2 (F2r) included an area 3 mm rostral to the genu of the arcuate sulcus in the posterior bank of the superior limb of the arcuate sulcus (Fig. 1D). Injection sites of the caudal sector of area F2 (F2c) included the area dorsal to the spur of the arcuate sulcus and below the superior precentral dimple (Fig. 1E). The viral suspension was injected through a 10-μL Hamilton microsyringe. For each injection track, viral deposits were placed at two different depths; at 4 and 2 mm deep from the cortical surface in F2r injections, and at 2 and 1.5 mm deep in F2c injections. At each depth, 0.5 μL of the viral suspension was deposited. When injections were complete, the dura mater and bone flap were repositioned, and the scalp incision was closed. An analgesic (Buprenex; 0.01 mg/kg, i.m.) was administered after surgery.

Histology

After a survival period of 3 or 4 days, the monkeys were deeply anesthetized with an overdose of sodium pentobarbital (50 mg/kg) and killed by perfusion-fixation with a mixture of 10% formalin and 15% saturated picric acid in 0.1 M phosphate buffer (pH 7.4). The

FIG. 2. Procedures to make two-dimensional density maps of the dentate nucleus and the interpositus nuclei of the macaque monkey. (A) Typical coronal sections of the dentate nucleus are displayed. The color-coded segments correspond to the colored regions on the unfolded map in (B). Each section is aligned to a junction between the 'a' and the 'b' segment (open stars). The 'a' segment is the lateral vertical segment of the nucleus, the 'b' segment is the main ventral segment and the 'c' segment is the medial vertical segment. (B) The broken line represents the border between the motor and the non-motor domain that was drawn following the convention of the cebus monkey (Strick *et al.*, 2009). Section numbers denoted above each plot in (A) correspond to the rostrocaudal positions depicted in (B). (C) Typical sections of the interpositus nuclei are displayed. (D) Each section is aligned to the top edge of the interpositus nuclei (open stars). Section numbers denoted below each plot in (C) correspond to the rostrocaudal positions depicted in (D). AIN, anterior interpositus nucleus; PIN, posterior interpositus nucleus.

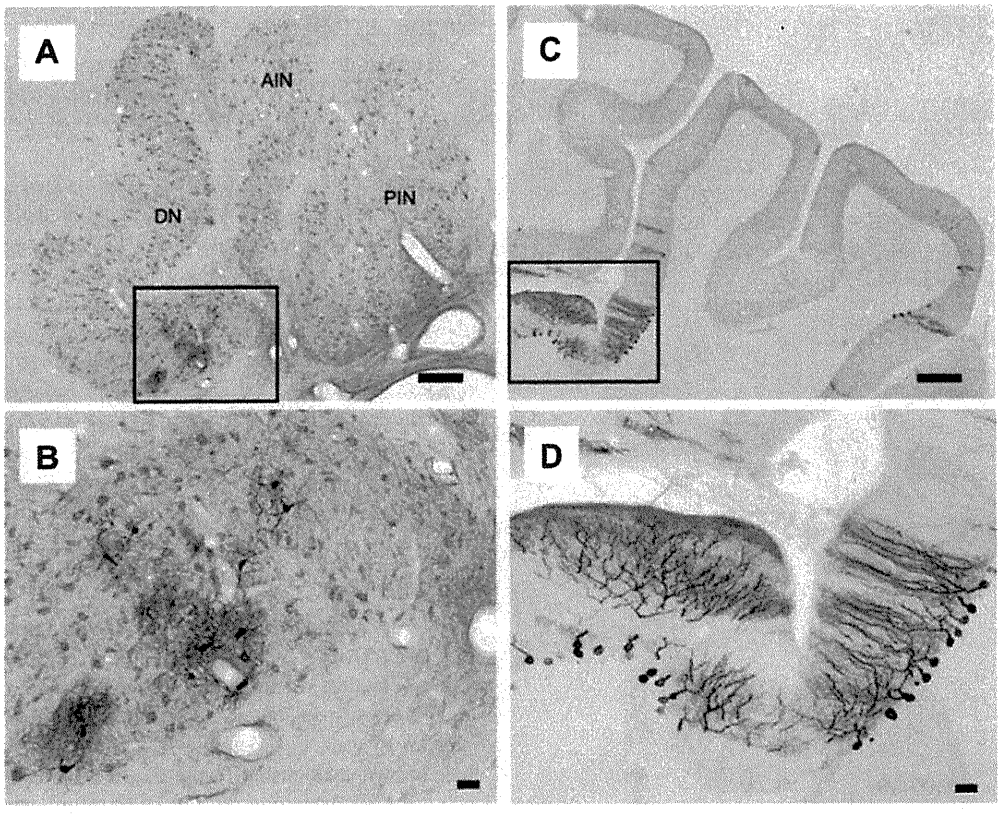

FIG. 3. Neuronal labeling in the cerebellum. (A) and (B) Second-order neuron labeling in the deep cerebellar nuclei 3 days after rabies injection into area F2. (A) Coronal section through the dentate (DN), anterior interpositus (AIN) and posterior interpositus (PIN) nuclei. The rectangular area in (A) is enlarged in (B). (C) and (D) Third-order labeling of Purkinje cells in the cerebellar cortex 4 days after rabies injection into area F2. (C) Coronal section through the lateral cerebellar hemisphere. The rectangular area in (C) is enlarged in (D). Scale bars: 500 μm (A and C); 50 μm (B and D).

brain was removed from the skull, postfixed in the same fresh fixative overnight at 4°C, and placed in 0.1 M phosphate buffer (pH 7.4) containing 30% sucrose. Coronal sections were cut serially at 50 μm thickness on a freezing microtome. Every sixth section was processed for immunohistochemical staining for rabies virus by means of the standard avidin-biotin-peroxidase complex method. Following immersion with 1% skim milk, the sections were incubated overnight with rabbit anti-rabies virus antibody in 0.1 M phosphate-buffered saline (pH 7.4) containing 0.1% Triton X-100 and 1% normal goat serum. The antibody was donated by Dr Satoshi Inoue (The National Institute of Infectious Disease, Tokyo, Japan). The sections were then placed in the same fresh incubation medium containing biotinylated goat anti-rabbit IgG antibody (diluted at 1 : 200; Vector Laboratories, Burlingame, CA, USA), followed by the avidin-biotin-peroxidase complex kit (ABC Elite; Vector Laboratories). For visualization of the antigen, the sections were reacted in 0.05 M Tris–HCl buffer (pH 7.6) containing 0.04% diaminobenzidine, 0.04% nickel chloride and 0.002% hydrogen peroxide.

TABLE 2. Numbers of labeled neurons in the deep cerebellar nuclei 3 days after rabies injections

Monkey, area and hemisphere	Dentate nucleus	Interpositus nucleus	Fastigial nucleus	Totals
Monkey Hyu, area F2r				
Contralateral	50	3	0	53
Ipsilateral	1	0	0	1
Monkey 06–23, area F2r				
Contralateral	66	48	0	114
Ipsilateral	1	2	0	3
Monkey Bei, area F2c				
Contralateral	1008	354	29	1391
Ipsilateral	14	12	5	31
Monkey Chi, area F2c				
Contralateral	404	166	137	707
Ipsilateral	9	6	6	21

Safety issues

The entire experiments were performed in a special primate laboratory (biosafety level 2) designated for *in vivo* virus experiments. Throughout the experiments, the monkeys were kept in individual cages that were installed inside a special safety cabinet. To avoid accidental infection with the virus, all investigators received immunization beforehand and wore protective clothing during the experimental sessions. Equipment was disinfected with 80% (v/v) ethanol after each experimental session and waste was autoclaved prior to disposal.

Analytical procedures

We digitized the outline of the deep cerebellar nuclei and the location of labeled neurons with the MD-Plot 3 system (Accustage, Shoreview, MN, USA) attached to a microscope system (Nikon Eclipse 80i, Tokyo, Japan). For the cerebellar cortex, we digitized its outline and

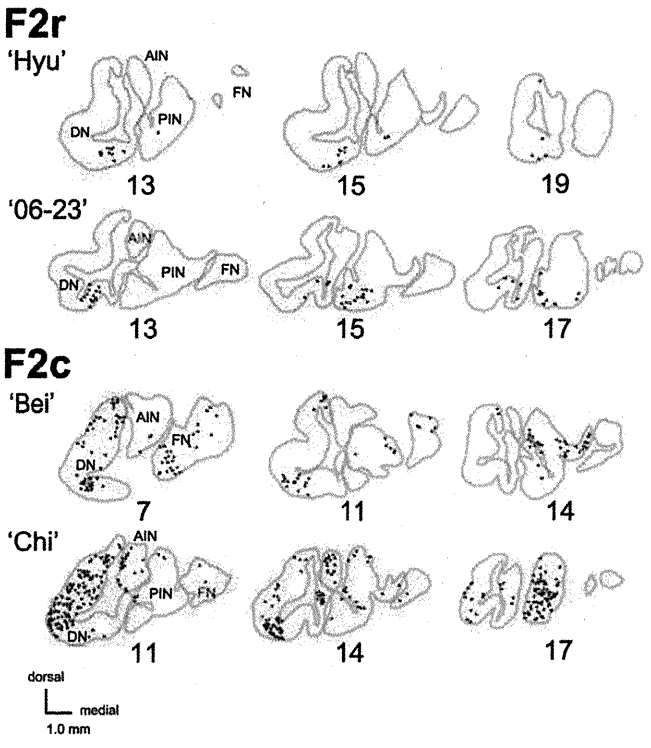

FIG. 4. Distributions of labeled neurons in the deep cerebellar nuclei. Three representative coronal sections are arranged rostrocaudally from left to right. Each row represents data in a single subject as identified by the label on the left. The top two rows are the cases of F2r injections, and the bottom two rows are the cases of F2c injections. Section numbers are indicated below each plot. The rostrocaudal positions are indicated by the inverted triangles in Fig. 5. Each dot indicates the location of one cell labeled by retrograde transneuronal transport (second-order neurons). Scale bar: 1 mm. AIN, anterior interpositus nucleus; DN, dentate nucleus; FN, fastigial nucleus; PIN, posterior interpositus nucleus.

the location of labeled neurons with Neurolucida (MBF Bioscience, Williston, VT, USA) attached to another microscope system (Nikon Eclipse 90i). Neuronal labeling was plotted on tracings of equidistant coronal sections (300 μm apart) through the deep cerebellar nuclei and the cerebellar cortex.

To examine the distribution and density of labeled neurons in the dentate nucleus, we made an unfolded map (two-dimensional density map) of the dentate nucleus by following the procedure reported by Dum & Strick (2003). For this purpose, we developed a program that runs on MATLAB (Mathworks, Natick, MA, USA). This program allowed us to load and display digitized data of each section, to put landmarks on the displayed section, and to draw a line onto which labeled neurons were projected. It further allowed us to align the positions of the projected neurons and landmarks across multiple sections. Using this program, we drew a curved line through the midway between the medial and lateral outline of the nucleus on each coronal section (Fig. 2A). The transitions between the major dentate segments and the position of each labeled neuron were projected onto the central line. Then, each line through the nucleus was unfolded and aligned on the transition between the 'a' segment (the lateral vertical segment of the nucleus) and the 'b' segment (the main ventral segment; Fig. 2B). To display the density of labeled neurons, we divided the unfolded map into 300 × 300-μm bins. We chose this dimension because we examined sections every 300 μm. A color code was assigned to each bin to indicate the number of labeled neurons it included. The only difference between Dum & Strick's method and ours is that we divided the dentate into three segments ('a', 'b' and 'c' segments) instead of five segments; the 'a' segment is the lateral vertical segment of the nucleus, the 'b' segment is the main ventral segment, and the 'c' segment is the medial vertical segment. This was because the shape of the dentate is slightly different between cebus and macaque monkeys. However, the alignment of the flattened map was made at the same point of the dentate nucleus.

To make a two-dimensional density map of the interpositus nuclei, we used the same custom-made program running on MATLAB. We first drew a vertical line passing through the interpositus nuclei on each coronal section (Fig. 2C). Markers indicating the dorsal and ventral edges of the nucleus and the position of each labeled neuron were projected onto the vertical line. Subsequently, each line through the nuclei was unfolded and aligned at the dorsal edge of the nuclei (Fig. 2D). To show the density of labeled neurons, we divided the unfolded map into 300 × 300-μm bins.

Results

In eight monkeys, multiple injections of rabies virus were made into F2r or F2c in the caudal PMd (Fig. 1A; Table 1). The injection sites were determined based on our previous electrophysiological studies, in which we recorded neuronal activity when monkeys were engaged in planning and executing an arm-reaching movement. We found that PMd activity reflecting the planning process was observed in an area lying between the border with the primary motor cortex and a region 3 mm rostral to the genu of the arcuate sulcus. Because saccadic eye movements were not evoked by intracortical microstimulation, we judged that this area corresponds to the caudal part of PMd (Fujii *et al.*, 2000), or area F2 (Matelli *et al.*, 1985, 1991). We further found that the functional properties were different in the rostral and caudal sectors of area F2; neurons in the rostral sector (F2r) medial to the genu of the arcuate sulcus were more responsive to motor instructions than those in the caudal sector (F2c) lateral to the superior precentral dimple (Fig. 1B). During the motor preparation period, F2r was characterized by activity reflecting the target location, irrespective of the arm use, whereas F2c was characterized by activity representing the arm use in conjunction with the target location (Fig. 1C; Hoshi & Tanji, 2006). This rostrocaudal segregation agrees with the classification made by analysing the anatomical connectivity (Matelli *et al.*, 1998; Luppino *et al.*, 2001, 2003). Based on these results, we determined the injection sites. For the F2r injection, we placed multiple injections at three points, i.e. at one point at the level of the genu of the arcuate sulcus and at two points ≤2 mm rostral to the genu (Fig. 1D). For the F2c injection, we placed multiple injections at four points (~1 mm apart) lateral to the superior precentral dimple (Fig. 1E). The extent of viral spread in each penetration is estimated to be < 0.5 mm in radius around the injection needle based on our prior study (see Fig. 3 in Miyachi *et al.*, 2005).

Three days after rabies injections into F2r or F2c, we found labeled neurons in the deep cerebellar nuclei mainly on the contralateral side (Fig. 3A and B; Table 2). These neurons, which probably reflected the second-order labeling, were viewed as sending projections contralaterally to F2r or F2c via the ventral thalamus. At this stage, however, we did not find labeled neurons in the cerebellar cortex. By extending the survival time up to 4 days, we observed third-order labeling of Purkinje cells in the cerebellar cortex (Fig. 3C and D). In the subsequent sections, we will describe the origins of the projections from the deep cerebellar nuclei and the cerebellar cortex.

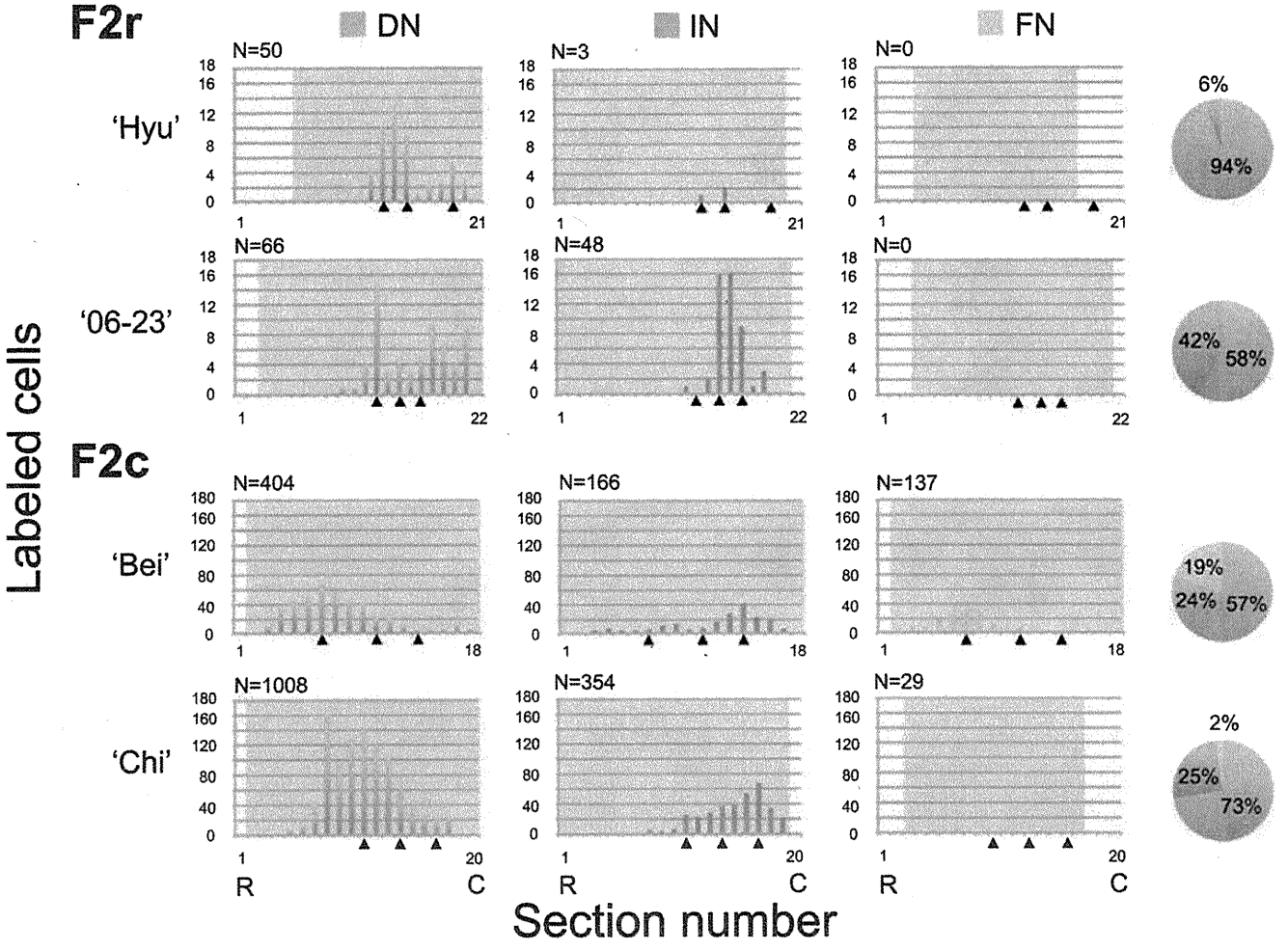

FIG. 5. Quantitative analyses of labeled neurons in the deep cerebellar nuclei. Left: histograms of the rostrocaudal distribution of labeled neurons in the deep cerebellar nuclei. The number was counted from plots of every sixth coronal section throughout the deep cerebellar nuclei. Each row summarizes data in a single subject as identified by the label on the left. The top two rows are the cases of F2r injections, and the bottom two rows are the cases of F2c injections. From left to right, data for the dentate nucleus (DN), the interpositus nuclei (IN) and fastigial nucleus (FN) are summarized. The gray areas indicate the extent of each nucleus. Right: pie charts showing the fraction of the number of labeled cells in the three nuclei. Blue, DN; Red, IN; Green, FN.

Origins of projections from the deep cerebellar nuclei to F2r and F2c

Dentate nucleus

We found that the distributions of labeled neurons after the F2r injections were different from those after the F2c injections. After the F2r injections, labeled neurons were found primarily in the caudo-ventral portion of the dentate nucleus (Figs 4–6). After the F2c injections, on the other hand, labeled neurons were located mainly in a more rostral and dorsal portion (Figs 4–6). The two-dimensional density map of the dentate nucleus summarizing the distribution of labeled neurons clearly illustrates that the neurons projecting to F2c tended to be distributed in the portion rostrodorsal to those projecting to F2r (Fig. 7). The number of labeled neurons was much greater after the F2c injections than after the F2r injections; the number of labeled neurons after the F2c injections was 706 on average (1008 and 404 cells for each monkey; Table 2), whereas the number of labeled neurons after the F2r injections was 58 on average (50 and 66 cells for each monkey; Table 2). To examine the extent of the area in which labeled neurons were distributed on the two-dimensional density map (Fig. 7), we calculated the proportion of bins containing labeled neurons to the total bins in the dentate nucleus. After the F2r injections, the proportion of bins with labeled neurons was 7% on average (25 out of 425 bins in Hyu, and 40 out of 482 bins in 06–23). After the F2c injections, on the other hand, the proportion of bins with labeled neurons was 42% on average (218 out of 427 bins in Chi, and 133 out of 392 bins in Bei). This analysis indicated that the labeled neurons in the dentate nucleus were sixfold more widely distributed after the F2c injections than after the F2r injections.

Interpositus nuclei

In each case of the F2r and F2c injections, labeled neurons in the interpositus nuclei were localized in the caudal portion (Fig. 5). To examine the distribution of the labeled neurons in detail, we made a two-dimensional density map of the interpositus nuclei (Fig. 8). We found that the difference in their distributions was seen along the dorsoventral axis; the F2r injections led to neuronal labeling mainly in the ventral portion, whereas the F2c injections led to broader neuronal labeling in both the dorsal and the ventral portions (Fig. 8). Further, the number of labeled neurons was much greater after the F2c injections than after the F2r injections; 260 cells on average (354 and

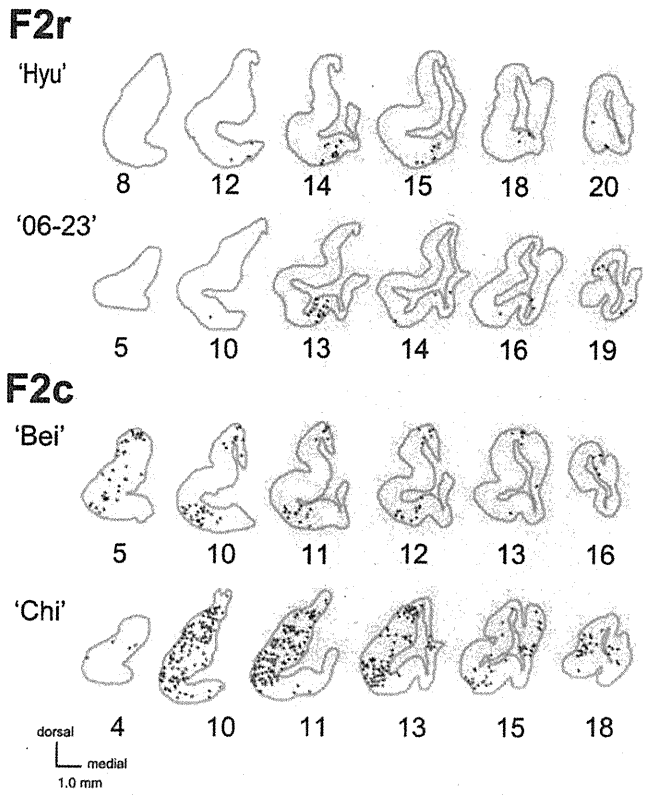

FIG. 6. Second-order neuron labeling in the dentate nucleus after virus injections into F2r or F2c. Six coronal sections are arranged rostrocaudally from left to right. Section numbers are indicated below each plot. Each dot indicates the location of one labeled cell. Each row summarizes data in a single subject as identified by the label on the left. The top two rows are the cases of F2r injections, and the bottom two rows are the cases of F2c injections. Scale bar: 1 mm.

166 cells for each monkey; Table 2) were labeled after the F2c injections, and 26 cells (3 and 48 cells for each monkey; Table 2) after the F2r injections. To examine the extent of the area in which labeled neurons were distributed on the two-dimensional density map (Fig. 8), we calculated the proportion of bins containing labeled neurons to the total bins. After the F2r injections, the proportion of bins with labeled neurons was 5% on average (2 out of 198 bins in Hyu, and 16 out of 175 bins in 06–23). After the F2c injections, on the other hand, the proportion of bins with labeled neurons was 39% on average (84 out of 178 bins in Chi, and 62 out of 196 bins in Bei). Thus, the labeled neurons in the interpositus nuclei were eightfold more widely distributed after the F2c injections than after the F2r injections.

Fastigial nucleus

After the F2r injections, virtually no neurons were labeled in the fastigial nucleus. A small number of labeled neurons were found after the F2c injections (29 and 137 cells for each monkey; Figs 4 and 5; Table 2).

Origins of projections from the cerebellar cortex to F2r and F2c

Four days after rabies injections into F2r and F2c, Purkinje cells in the cerebellar cortex were labeled (Fig. 3C and D). After the F2r injections, only a small number of labeled Purkinje cells were found in Crus I and II of the lateral hemisphere (75 and 65 cells for each monkey; top row in Fig. 9). By contrast, after the F2c injections, labeled Purkinje cells were more numerous (4144 and 3251 cells for each monkey) and distributed broadly over the lateral hemisphere, including lobules III–VI, VIIB and VIII (3144 and 1590 cells for each monkey; bottom row in Fig. 9), and Crus I and II (1000 and 1661 cells for each monkey).

Discussion

In this study, we applied retrograde transsynaptic transport of a neurotropic virus in macaque monkeys to examine the origins of cerebellar projections to distinct sectors in the caudal PMd (area F2). We have found that the rostral sector (F2r) and the caudal sector (F2c) receive inputs from distinct portions of the deep cerebellar nuclei and the cerebellar cortex.

Projections from the cerebellum to the PMd

A series of studies conducted by Strick *et al.* have demonstrated the existence of two distinct territories in the dentate nucleus. The rostral and dorsal portion, named the motor domain, contains output channels that innervate the primary motor cortex, supplementary motor area and ventral premotor cortex of the frontal lobe (Fig. 2B; Dum & Strick, 1991, 2003; Hoover & Strick, 1999; Akkal *et al.*, 2007; Lu *et al.*, 2007). By contrast, the caudal and ventral portion of the dentate nucleus, named the non-motor domain, contains output channels that innervate the prefrontal cortex (lateral area 9 and dorsal area 46), presupplementary motor area and area 7b in the posterior parietal cortex (Middleton & Strick, 1994, 2001; Clower *et al.*, 2001; Akkal *et al.*, 2007). By comparing our results with previous reports (Dum & Strick, 2003) based on the flattened map of the dentate nucleus (Fig. 7), it has been revealed that the projections to F2r originate predominantly from the non-motor domain, whereas those to F2c arise mainly from the motor domain. However, we raise two important issues. First, although we found labeled neurons in the 'c' segment (Fig. 2B) of some monkeys, the target of this segment has not yet been examined systematically. Second, the exact border between the motor and the non-motor domain has not been determined in macaque monkeys. Although these issues do not necessarily affect the interpretation of our results, they should be solved in the near future to analyse the structural organization of the macaque dentate nucleus in more detail.

In the interpositus nuclei, the cellular origin of the projections to F2c was more widely distributed, while that of the projections to F2r was restricted mainly to the caudal and ventral portion. These results suggest that the interpositus nuclei may consist of functionally separate zones, each of which is interconnected with distinct sectors of PMd. In addition, we found that the fastigial nucleus projects to F2c only. Taken together, the present data have shown that the medial aspects of the deep cerebellar nuclei send projections to F2c rather than F2r.

In the cerebellar cortex, it has been demonstrated that the prefrontal cortex and the primary motor cortex are linked with distinct zones (Kelly & Strick, 2003; Lu *et al.*, 2007); lobules IV–VI, VIIB and VIII are linked with the arm area of the primary motor cortex, whereas Crus II is linked with area 46 in the prefrontal cortex. The present study has shown that F2r receives input from Purkinje cells located in Crus II as well as in Crus I. By contrast, F2c receives input from Purkinje cells located in lobules III–VIII, including Crus I and Crus II. Although Crus II projects to both F2r and F2c, it still remains to be known whether there are separate channels, each of which is interconnected with F2r or F2c. From this point of view, the densest zones of cellular origin to F2r and F2c were segregated rostrocaudally in the ventral aspect of the dentate nucleus (Fig. 7), suggesting that F2r and F2c receive cerebellocerebral inputs from Crus II via distinct channels.

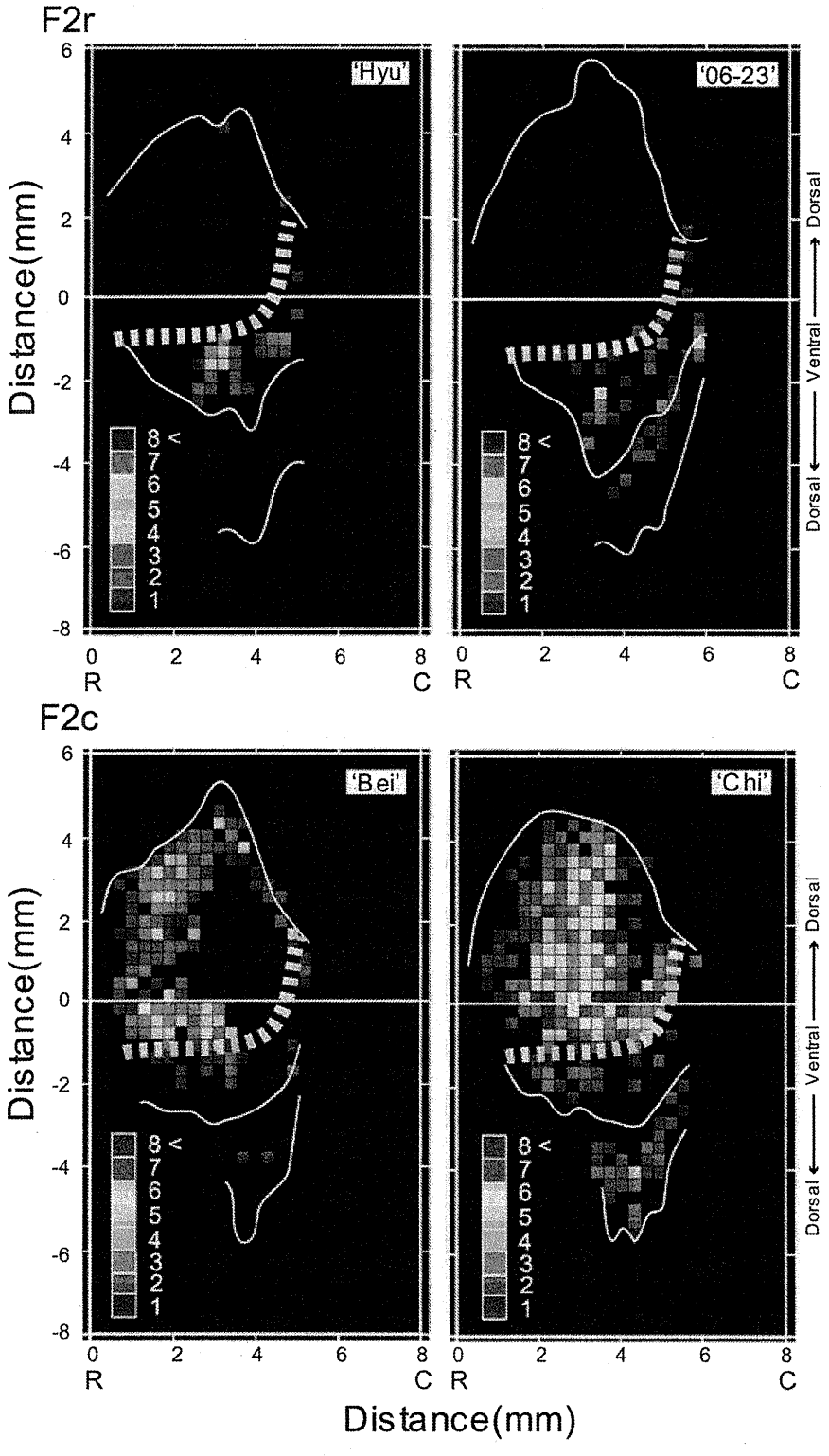

FIG. 7. Two-dimensional density maps of the dentate nucleus of the macaque monkey. Distribution and density of labeled dentate cells projecting to F2r and F2c are displayed on an unfolded map of the dentate nucleus (for the procedures, see Materials and methods; see also Fig. 2A and B). The color code in the bottom left of each panel indicates the number of labeled neurons in each bin (300 × 300 μm). The maps were reconstructed from plots of every sixth coronal section (50 μm thickness) throughout the dentate nucleus. The top row shows the results of F2r injections, and the bottom row shows the results of F2c injections. The identity of each subject is indicated at the top right of each panel. C, caudal; R, rostral. In each panel, the broken line represents the border between the regions that contain bins having and not having dense projections to F2r in the main ventral segment (see 'b' in Fig. 1B).

Our results may be at odds with those reported by Strick et al., indicating that only the motor domain of the deep cerebellar nuclei projects to the caudal PMd that corresponds probably to both F2r and F2c (see Introduction). However, the difference in the distribution of cerebellar origin can be explained by the fact that they injected rabies virus into the digit region of PMd, while we injected the virus into the

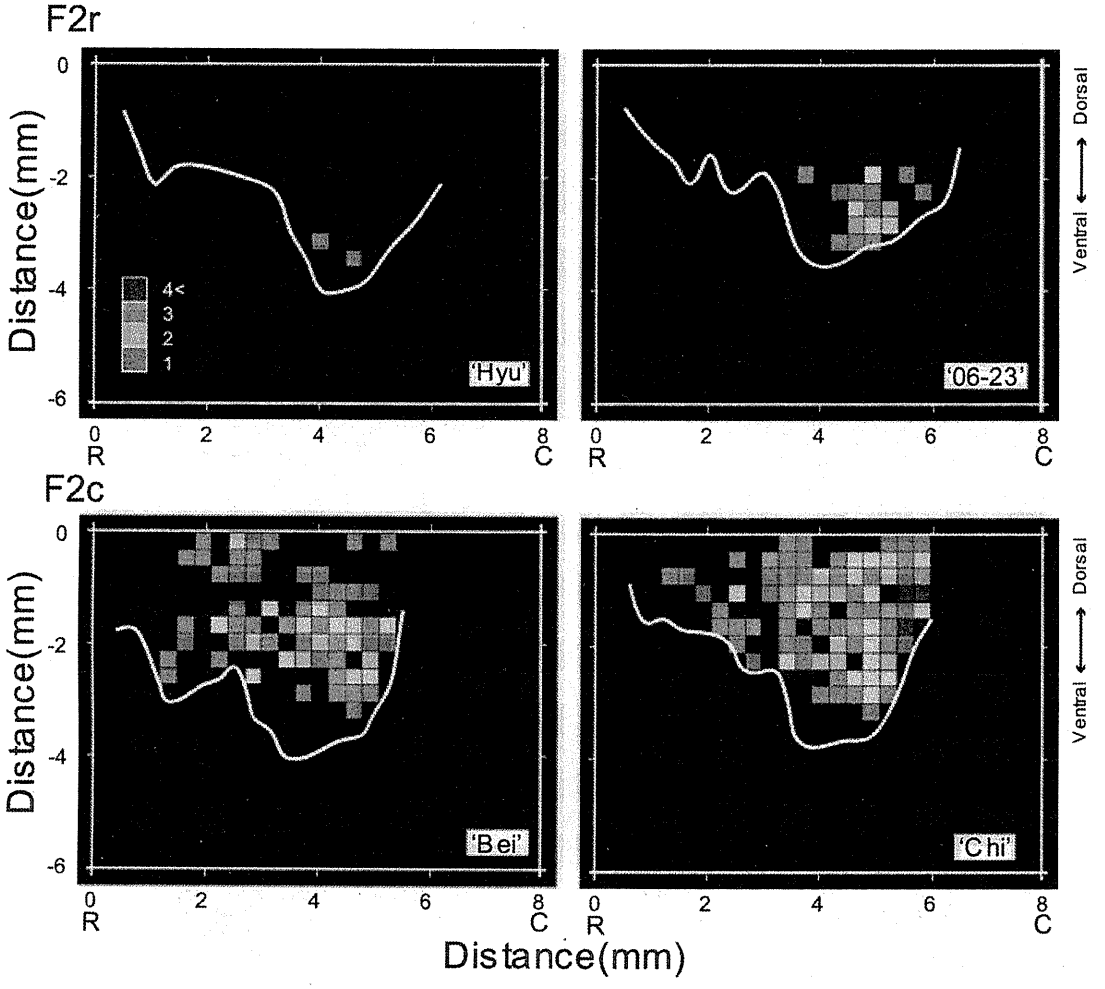

FIG. 8. Two-dimensional density maps of the interpositus nuclei of the macaque monkey. Distribution and density of labeled interpositus cells projecting to F2r and F2c are displayed on an unfolded map of the interpositus nuclei (for the procedures, see Materials and methods; see also Fig. 2C and D). The color code in the bottom left of each panel indicates the number of labeled neurons in each bin (300 × 300 μm). The maps were reconstructed from plots of every sixth coronal section (50 μm thickness) throughout the interpositus nuclei. The top row shows the results of F2r injections, and the bottom row shows the results of F2c injections. The identity of each subject is indicated at the bottom right of each panel. C, caudal; R, rostral.

shoulder region of PMd where visuomotor transformation for reaching behavior is carried out (Caminiti *et al.*, 1991; Wise *et al.*, 1997). Because hand action is suggested to depend on neural mechanisms largely different from arm reach (Jeannerod *et al.*, 1995), the apparent disparity could be ascribed to the difference in the target site of rabies injection.

We found that deep cerebellar neurons labeled after the F2c injections were more numerous than after the F2r injections. Overall, neuronal labeling from F2c was 12-fold denser in the dentate nucleus and 10-fold denser in the interpositus nuclei than that from F2r. We here consider two factors that are deemed to account for such a great difference. First, examination of the areas containing labeled neurons on the two-dimensional density maps (Figs 7 and 8) revealed that the area projecting to F2c was sixfold larger in the dentate nucleus and eightfold larger in the interpositus nuclei than that projecting to F2r. Second, the total injection volume was somewhat different in the cases of F2r injections (3 μL) and F2c injections (4 μL). When we analysed the patterns of neuronal labeling in the ventral thalamic nuclei at the 3-day post-injection period, we found that the thalamic neurons were densely (to almost the same extent) labeled in each of the injection cases. This indicates that the virus was transported retrogradely with similar efficacy. Taken together, these two observations suggest that the difference in the total number of labeled neurons originates mainly from the difference in the size of the area containing projection neurons (i.e. the intensity of the projection) and, additionally, from the difference in the total viral uptake. In the future, it will be necessary to inject distinct transneuronal tracers into each of F2r and F2c in a single subject to obtain quantitatively more accurate data (e.g. Ohara *et al.*, 2009).

Functional roles of cerebellar projections to F2r and F2c

Leiner *et al.* (1986) proposed that the phylogenetically latest structures of the cerebellum, i.e. the ventrolateral dentate nucleus and the lateral cerebellar hemisphere, develop in parallel with the association areas in the cerebral cortex. These findings provide anatomical evidence for a view that the cerebellum is involved not only in controlling motor acts (Soechting *et al.*, 1976; Thach *et al.*, 1992; Asanuma & Pavlides, 1997; Kleim *et al.*, 1997; Lu *et al.*, 1998; Thach, 1998; Nixon & Passingham, 2000), but also in higher-order brain functions; the involvement of the cerebellum in various aspects of non-motor functions has been shown by human imaging studies (Petersen *et al.*, 1988; Ryding *et al.*, 1993; Kim *et al.*, 1994; Raichle *et al.*, 1994; Fiez *et al.*, 1996; Gao *et al.*, 1996; Allen *et al.*, 1997; Jueptner *et al.*, 1997a,b), clinical case studies

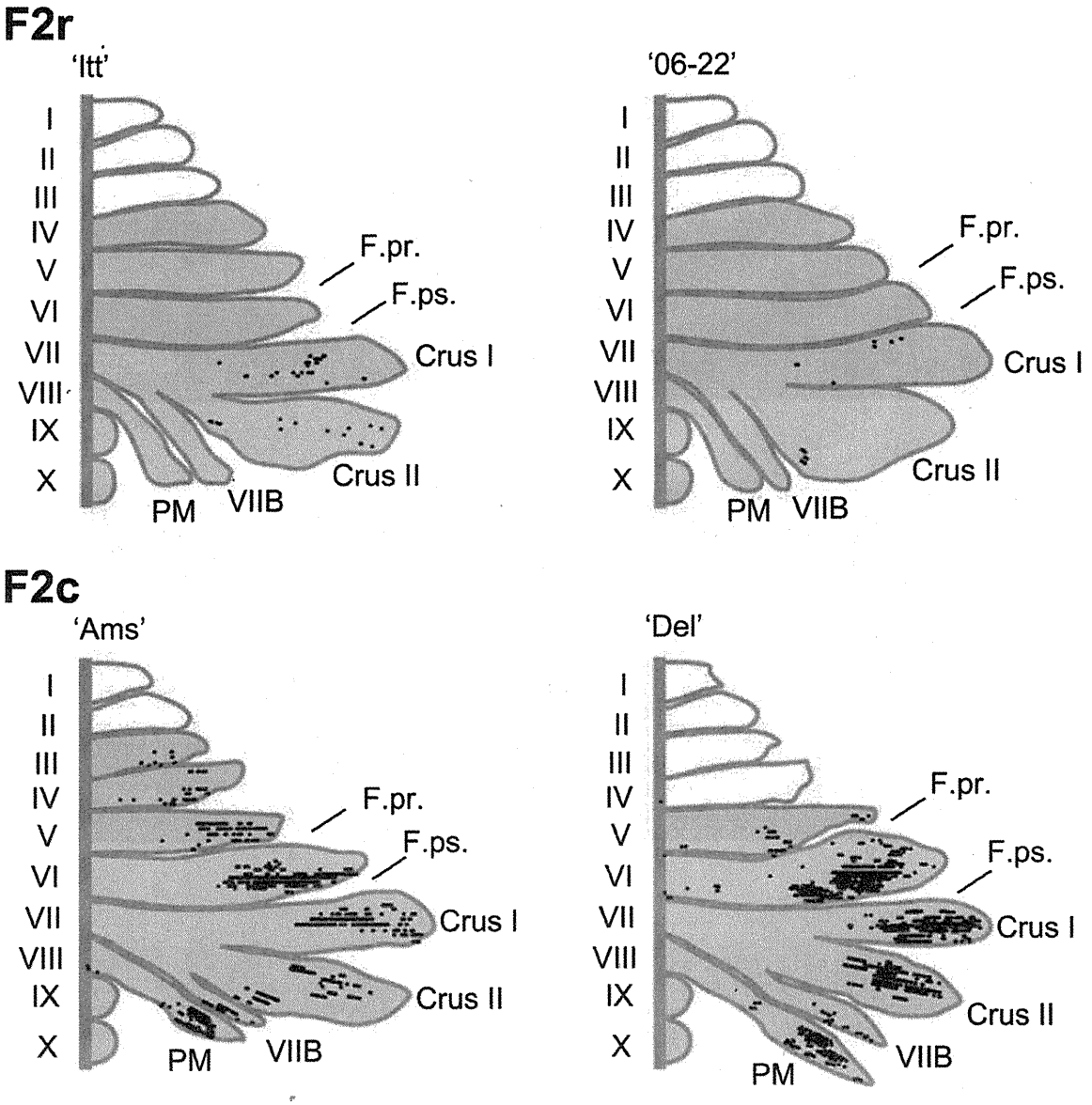

FIG. 9. Reconstruction of Purkinje cell labeling in the cerebellar hemisphere. Each dot indicates one cell labeled after rabies injections into F2r (top row) or F2c (bottom row). The gray areas indicate cerebellar cortical regions through which coronal sections could be retrieved and analysed. F.pr, primary fissure; F.ps, posterior superior fissure; PM, paramedian lobule.

(Fiez *et al.*, 1992; Grafman *et al.*, 1992; Courchesne *et al.*, 1995; Schmahmann & Pandya, 1997; Schmahmann & Sherman, 1998) and structural analyses (Paradiso *et al.*, 1997). We here demonstrated that the lateral aspect of the cerebellar cortex projects to both F2r and F2c. The network might play a role in motor planning or sensorimotor transformation beyond the movement execution itself.

By examining single-neuron activity of the dentate nucleus while monkeys performed a motor task, it has been shown that neurons in the ventral part of the dentate nucleus are not activated in relation to limb movements (Thach, 1978; Wetts *et al.*, 1985), consistent with the fact that this area corresponds to the non-motor domain. More recently, Mushiake & Strick (1993) recorded neuronal activity from the ventral part of the dentate nucleus in monkeys performing sequential reaching movements and reported that neuronal activity during the instruction-delay period was selective for a particular sequence of movements. Subsequently, Ohbayashi *et al.* (2003) showed that PMd was involved in planning sequential movements. With respect to the control of bimanual movements, it has been revealed that Purkinje cells in the lateral cerebellar hemisphere (lobules IV–VII including Crus I and II) and a subset of PMd neurons, especially in F2r, discharge in a similar manner, no matter which arm (left or right) is used (Cisek *et al.*, 2003; Greger *et al.*, 2004; Hoshi & Tanji, 2006). Thus, these results suggest that PMd and the cerebellum may be both involved in higher-order aspects of motor behavior, such as sequencing multiple movements and controlling bimanual motor acts. Our recent study indicates that PMd transforms an abstract representation of motor act into its physical representation that can be executed as a movement (Nakayama *et al.*, 2008). It is most likely that such a transformation process may be achieved partly through the interaction with the cerebellum.

By contrast, it has been reported that the cerebellum is not involved in transforming object identity information into a directional motor signal in conditional motor behavior (Nixon & Passingham, 2000), which is consistent with the evidence that the inferior temporal cortex involved in object recognition (Mishkin *et al.*, 1983) does not project to the cerebellum (Glickstein *et al.*, 1985). Thus, the involvement of

the cerebellum in the cognitive control of behavior is not universal. Given that PMd retrieves a motor instruction associated with visual object without selectivity for the object identity itself (Hoshi & Tanji, 2000, 2006, 2007; Yamagata *et al.*, 2009), it can be construed that the cerebellum and PMd are posited at similar hierarchic levels for visuomotor transformation. Very recently, Prevosto *et al.* (2010) examined the cerebellocerebral projections to the medial intraparietal area (MIP), which is interconnected with PMd (Matelli *et al.*, 1998; Caminiti *et al.*, 1999). This study has demonstrated that MIP receives inputs from the ventral region of the dentate nucleus and Crus II of the cerebellar cortex; these regions coincide well with those projecting to F2r and F2c. This raises an intriguing possibility that the cerebellum may play a central role in transformation of visuospatial information into a motor command (Pesaran *et al.*, 2006; Batista *et al.*, 2007) in cooperation with PMd and MIP.

The present study has revealed that the motor domain of the cerebellum projects almost exclusively to F2c; the rostral and dorsal portion of the dentate nucleus, the interpositus nuclei, the fastigial nucleus, and lobules III–VIII of the cerebellar cortex send outputs to F2c. Physiological studies have shown that F2c neurons display prominent movement-related activity as well as set-related activity before movement initiation (Weinrich & Wise, 1982; Wise, 1985; Wise & Mauritz, 1985; Kurata & Wise, 1988; Kurata, 1993). Thus, these types of motor activity might be generated, at least in part, through the interaction with the cerebellum as is the case for the primary motor cortex (Holdefer *et al.*, 2000).

In summary, the present results have demonstrated that the rostrally located F2r and the caudally located F2c in the caudal PMd receive their main inputs from distinct zones of the cerebellum. F2c receives input mainly from the motor domain of the cerebellum, whereas F2r receives input from the non-motor domain of the cerebellum. Further investigations are necessary to clarify the anatomical organization and functional interactions between the cerebellum and PMd.

Acknowledgements

We wish to thank Dr P.L. Strick for providing invaluable comments on this manuscript. We are grateful to M. Imanishi, Y. Ito, T. Kuroda, E. Mine, T. Ogata and Dr K. Samejima for technical assistance. This work was supported by Grants-in-Aid for Scientific Research on Priority Areas (Integrative Brain Research) from the Ministry of Education, Culture, Sports, Science and Technology of Japan (20019027 to E.H., 17021050 to M.T.), a Grant-in-Aid for Young Scientists (S) from Japan Society for the Promotion of Science (19670004 to E.H.), and a Career Development Award from the International Human Frontier Science Program Organization (E.H.).

Abbreviations

MIP, medial intraparietal area; PMd, dorsal premotor cortex.

References

Akkal, D., Dum, R.P. & Strick, P.L. (2007) Supplementary motor area and presupplementary motor area: targets of basal ganglia and cerebellar output. *J. Neurosci.*, **27**, 10659–10673.

Allen, G., Buxton, R.B., Wong, E.C. & Courchesne, E. (1997) Attentional activation of the cerebellum independent of motor involvement. *Science*, **275**, 1940–1943.

Asanuma, H. & Pavlides, C. (1997) Neurobiological basis of motor learning in mammals. *Neuroreport*, **8**, i–vi.

Barbas, H. & Pandya, D.N. (1987) Architecture and frontal cortical connections of the premotor cortex (area 6) in the rhesus monkey. *J. Comp. Neurol.*, **256**, 211–228.

Batista, A.P., Santhanam, G., Yu, B.M., Ryu, S.I., Afshar, A. & Shenoy, K.V. (2007) Reference frames for reach planning in macaque dorsal premotor cortex. *J. Neurophysiol.*, **98**, 966–983.

Brodmann, K. (1909). *Vergleichende Lokalisationslehre der Grobhirnrinde.* Barth, Leipzig.

Callaway, E.M. (2008) Transneuronal circuit tracing with neurotropic viruses. *Curr. Opin. Neurobiol.*, **18**, 617–623.

Caminiti, R., Johnson, P.B., Galli, C., Ferraina, S. & Burnod, Y. (1991) Making arm movements within different parts of space: the premotor and motor cortical representation of a coordinate system for reaching to visual targets. *J. Neurosci.*, **11**, 1182–1197.

Caminiti, R., Genovesio, A., Marconi, B., Mayer, A.B., Onorati, P., Ferraina, S., Mitsuda, T., Giannetti, S., Squatrito, S., Maioli, M.G. & Molinari, M. (1999) Early coding of reaching: frontal and parietal association connections of parieto-occipital cortex. *Eur. J. Neurosci.*, **11**, 3339–3345.

Cisek, P., Crammond, D.J. & Kalaska, J.F. (2003) Neural activity in primary motor and dorsal premotor cortex in reaching tasks with the contralateral versus ipsilateral arm. *J. Neurophysiol.*, **89**, 922–942.

Clower, D.M., West, R.A., Lynch, J.C. & Strick, P.L. (2001) The inferior parietal lobule is the target of output from the superior colliculus, hippocampus, and cerebellum. *J. Neurosci.*, **21**, 6283–6291.

Clower, D.M., Dum, R.P. & Strick, P.L. (2005) Basal ganglia and cerebellar inputs to 'AIP'. *Cereb. Cortex*, **15**, 913–920.

Courchesne, E., Akshoomoff, N.A., Townsend, J. & Saitoh, O. (1995) A model system for the study of attention and the cerebellum: infantile autism. *Electroencephalogr. Clin. Neurophysiol. Suppl.*, **44**, 315–325.

Dum, R.P. & Strick, P.L. (1991) The origin of corticospinal projections from the premotor areas in the frontal lobe. *J. Neurosci.*, **11**, 667–689.

Dum, R.P. & Strick, P.L. (2003) An unfolded map of the cerebellar dentate nucleus and its projections to the cerebral cortex. *J. Neurophysiol.*, **89**, 634–639.

Dum, R.P., Li, C. & Strick, P.L. (2002) Motor and nonmotor domains in the monkey dentate. *Ann. N Y Acad. Sci.*, **978**, 289–301.

Dum, R.P., Akkal, D. & Strick, P.L. (2004) *The Dorsal Premotor Area (PMd) and the Pre-PMd Area are the Target of Basal Ganglia and Cerebellar Output in the Cebus Monkey.* Program No. 535.12. 2004 Neuroscience Meeting Planner. San Diego, CA, Society for Neuroscience. Online.

Fiez, J.A., Petersen, S.E., Cheney, M.K. & Raichle, M.E. (1992) Impaired non-motor learning and error detection associated with cerebellar damage. A single case study. *Brain*, **115**(Pt 1), 155–178.

Fiez, J.A., Raife, E.A., Balota, D.A., Schwarz, J.P., Raichle, M.E. & Petersen, S.E. (1996) A positron emission tomography study of the short-term maintenance of verbal information. *J. Neurosci.*, **16**, 808–822.

Fujii, N., Mushiake, H. & Tanji, J. (2000) Rostrocaudal distinction of the dorsal premotor area based on oculomotor involvement. *J. Neurophysiol.*, **83**, 1764–1769.

Gao, J.H., Parsons, L.M., Bower, J.M., Xiong, J., Li, J. & Fox, P.T. (1996) Cerebellum implicated in sensory acquisition and discrimination rather than motor control. *Science*, **272**, 545–547.

Glickstein, M., May, J.G. 3rd & Mercier, B.E. (1985) Corticopontine projection in the macaque: the distribution of labelled cortical cells after large injections of horseradish peroxidase in the pontine nuclei. *J. Comp. Neurol.*, **235**, 343–359.

Grafman, J., Litvan, I., Massaquoi, S., Stewart, M., Sirigu, A. & Hallett, M. (1992) Cognitive planning deficit in patients with cerebellar atrophy. *Neurology*, **42**, 1493–1496.

Greger, B., Norris, S.A. & Thach, W.T. (2004) Spike firing in the lateral cerebellar cortex correlated with movement and motor parameters irrespective of the effector limb. *J. Neurophysiol.*, **91**, 576–582.

Holdefer, R.N., Miller, L.E., Chen, L.L. & Houk, J.C. (2000) Functional connectivity between cerebellum and primary motor cortex in the awake monkey. *J. Neurophysiol.*, **84**, 585–590.

Hoover, J.E. & Strick, P.L. (1999) The organization of cerebellar and basal ganglia outputs to primary motor cortex as revealed by retrograde transneuronal transport of herpes simplex virus type 1. *J. Neurosci.*, **19**, 1446–1463.

Hoshi, E. & Tanji, J. (2000) Integration of target and body-part information in the premotor cortex when planning action. *Nature*, **408**, 466–470.

Hoshi, E. & Tanji, J. (2006) Differential involvement of neurons in the dorsal and ventral premotor cortex during processing of visual signals for action planning. *J. Neurophysiol.*, **95**, 3596–3616.

Hoshi, E. & Tanji, J. (2007) Distinctions between dorsal and ventral premotor areas: anatomical connectivity and functional properties. *Curr. Opin. Neurobiol.*, **17**, 234–242.

Ito, M. (1984). *The Cerebellum and Neural Control.* Raven, New York.

Jeannerod, M., Arbib, M.A., Rizzolatti, G. & Sakata, H. (1995) Grasping objects: the cortical mechanisms of visuomotor transformation. *Trends Neurosci.*, **18**, 314–320.